ENVISAT GOMOS Monthly report: October 2003

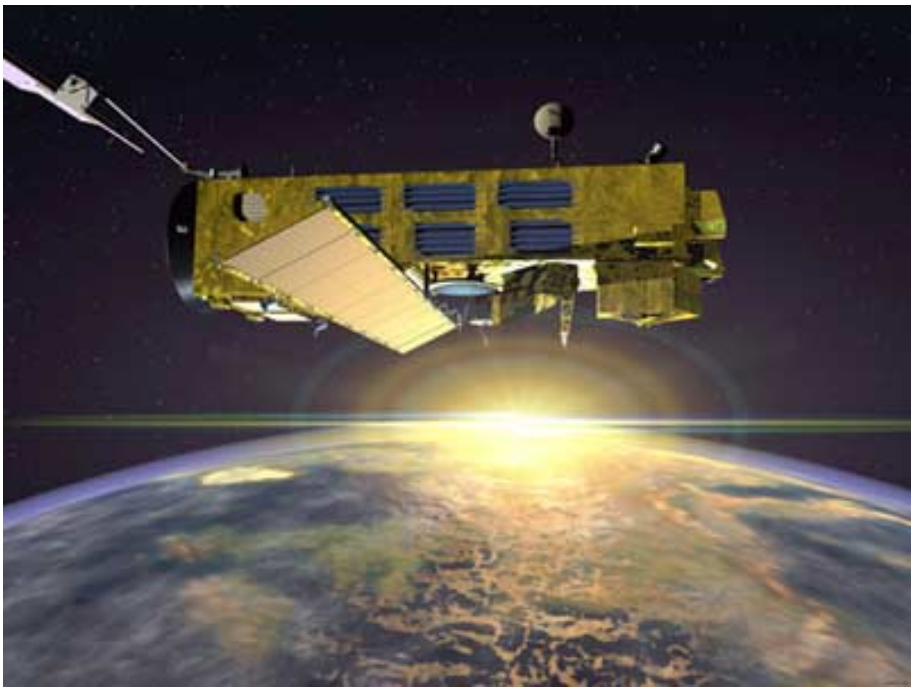

Prepared by:	PCF team	ESA EOP-GOQ
Inputs from:	GOMOS Quality Working Group	
Issue:	1.0	
Reference:	ENVI-SPPA-EOPG-TN-03-0029	
Date of issue:	27 Nov. 03	
Status:	Reviewed	
Document type:	Technical Note	
Approved by:	Pascal Lecomte, Rob Koopman	

TABLE OF CONTENTS

1 INTRODUCTION

The GOMOS monthly report documents the current status and recent changes to the GOMOS instrument, its data processing chain, and its data products.
The Monthly Report (hereafter MR) is composed of analysis results obtained by the Product Control Facility, combined with inputs received from the different entities working on GOMOS operation, calibration, product validation and data quality. These teams participate in the GOMOS Quality Working Group:

- European Space Agency (ESRIN-PCF, ESOC, ESTEC-PLSO)
- ACRI
- Service d'Aeronomie
- Finnish Meteorological Institute
- IASB-Belgian Institute for Space Aeronomy
- Atrium Space
- ECMWF

In addition, the group interfaces with the Atmospheric Chemistry Validation Team.

1.1 Scope

The main objective of the Monthly Report is to give, on a regular basis, the status of GOMOS instrument performance, data acquisition, results of anomaly investigations, calibration activities and validation campaigns. The following six sections compose the MR:

- Summary
- Unavailability
- Instrument Performance and Configuration
- Level 1 Product Quality Monitoring
- Level 2 Product Quality Monitoring
- Validation Activities and Results

1.2 References

[1] ENVISAT Weekly Mission Operations Report #71, #72, #73, #74, #75 ENVI-ESOC-OPS-RP-1011-TOS-OF
[2] 'Level 1b Detailed Processing Model', PO-RS-ACR-GS-0001, issue 5.4, 20 Nov, 2002
[3] 'Level 2 Detailed Processing Model', PO-RS-ACR-GS-0002, issue 5.4, 20 Nov, 2002

1.3 Acronyms and abbreviations

ACVT	Atmospheric Chemistry Validation Team
ADF	Auxiliary Data File
ADS	Auxiliary Data Server
ANX	Ascending Node Crossing
ARF	Archiving Facility (PDS)
CCU	Central Communication Unit
CFS	CCU Flight Software
CNES	Centre National d'Études Spatiales
CTI	Configuration Table Interface
CR	Cyclic Report
DC	Dark Charge
DMOP	Detailed Mission Operation Plan
DPM	Detailed Processing Model
DS	Data Server
DSA	Dark Sky Area
DSD	Data Set Descriptor
ECMWF	European Centre for Medium Weather Forecast
EQSOL	Equipment Switch Off Line
ESA	European Space Agency
ESRIN	European Space Research Institute
ESTEC	European Space Research & Technology Centre
ESOC	European Space Operations Centre
FCM	Fine Control Mode
FMI	Finnish Meteorological Institute
FOCC	Flight Operations Control Centre (ENVISAT)
FP1	Fast Photometer 1
FP2	Fast Photometer 2
GOMOS	Global Ozone Monitoring by Occultation of Stars
GOPR	GOmos PRototype
GS	Ground Segment
HK	Housekeeping
IASB	Institut d'Aeronomie Spatiale de Belgique
IAT	Interactive Analysis Tool
ICU	Instrument Control Unit
IDL	Interactive Data Language
IECF	Instrument Engineering and Calibration Facilities
IMK	Institute of Meteorology Karlsruhe (Meteorologisch Institut Karlsuhe)
INV	Inventory Facilities (PDS)
IPF	Instrument Processing Facilities (PDS)
JPL	Jet Propulsion Laboratory
LAN	Local Area Network
LPCE	Laboratoire de Physique et Chimie de l'Environnement
LUT	Look Up Table
MCMD	Macro Command
MDE	Mechanism Drive Electronics
MIP	Most Illuminated Pixel

MPH	Main Product Header
MR	Monthly Report
OBT	On Board Time
OCM	Orbit Control Manoeuvre
OOP	Out-of-plane
OP	Operational Phase of ENVISAT
PAC	Processing and Archiving Centre (PDS)
PCF	Product Control Facility
PDCC	Payload Data Control Centre (PDS)
PDHS	Payload Data Handling Station (PDS)
PDHS-E	Payload Data Handling Station – ESRIN
PDHS-K	Payload Data Handling Station – Kiruna
PDS	Payload Data Segment
PLSOL	Payload Switch off Line
PMC	Payload Module Computer
PRNU	Pixel Response Non Uniformity
QC	Quality Control
QUARC	Quality Analysis and Reporting Computer
QWG	Quality Working Group
RIVM	Rijksinstituut voor Volksgezondheid en Milieu
RTS	Random Telegraphic Signal
SA	Service d'Aeronomie
SATU	Star Acquisition and Tracking Unit
SFCM	Stellar Fine Control Mode
SFM	Steering Front Mechanism
SMNA	Servicio Meteorológico Nacional de Argentina
SODAP	Switch On and Data Acquisition Phase
SPA1	Spectrometer A CCD 1
SPA2	Spectrometer A CCD 2
SPB1	Spectrometer B CCD 1
SPB2	Spectrometer B CCD 2
SPH	Specific Product Header
SQADS	Summary Quality Annotation Data Set
SSP	Sun Shade Position
SZA	Solar Zenith Angle

2 SUMMARY

The GOMOS instrument has been operating nominally during the reporting month. Due to an out-of-plane manoeuvre scheduled for 28th October GOMOS was unavailable the whole day (until 06:00 of the day after) and few hours on 31st (section 3.1).

There was an OBT wrap-around on 4th October and the commanding for all instruments and PEB were avoided during the event period.

The availability of level 1b data within the archives is quite stable around 97% during the whole month of October. Also the level 0 availability is stable being the percentage situated almost at 99% (section 3.3).

The temperature behaviour of the detectors is nominal within the reporting period. The expected seasonal variation of the temperatures with amplitude of around one degree can be observed (section 4.2).

The elevation at which stars first appear on the star-tracking detector shows significant deviation in elevation from the expected position. Stars now initially appear above the SATU elevation centre. The variation in this MIP positions displays seasonal variation and is an indicator of an ENVISAT platform attitude deviation (section 4.5.3).

The variation of the radiometric sensitivity ratio is outside the threshold for some photometer ratios and for some stars. Investigation results will be reported in future monthly reports (section 5.4.1).

On 10th, 21st and 30th October new calibration ADF's were disseminated with updated DC map of orbits 08413, 08555 and 08695 respectively.

ESA has continued the supply of selected data products to validation teams using the prototype processor at ACRI. An upgrade of the data processing algorithm specification is in progress, in order to improve both level 1 and level 2 products.

3 INSTRUMENT UNAVAILABILITY

3.1 GOMOS unavailability periods

In table 3.1-1 there is a list of GOMOS unavailability reports issued during the period 1st October (00:00:00) 2003 until 31st October (24:00:00) 2003. No anomalies occurred to GOMOS during October being the two unavailabilities related to an Orbit Control Manoeuvre and hence, planned.

Table 3.1-1 List of unavailability reports issued during October

Reference of unavailability report	Start time Star orbit	Stop time Stop orbit	Description
EN-UNA-2003/0316	28 Oct 2003 02:55:00.000 Day of Year = 301 Orbit = 08675 Anx Offset = 0823.991	29 Oct 2003 06:00:00.000 Day of Year = 302 Orbit = 08691 Anx Offset = 1749.143	Planned: Instrument commanded into required mode for the scheduled OCM and CFS patch.
EN-UNA-2003/0317	30 Oct 2003 23:35:00.000 Day of Year = 303 Orbit = 08716 Anx Offset = 0550.943	31 Oct 2003 02:27:00.000 Day of Year = 304 Orbit = 08717 Anx Offset = 4835.015	Planned: Interruption of instrument operations due to a planned FCM

3.2 Stars lost in centering

The acquisition of a star initiates with a rallying phase where the telescope mechanism is directed towards the expected position of the star. Subsequently the acquisition procedure enters into detection mode, where the SATU star tracker output signal is pre-processed for spot presence survey and for the location of the most illuminated couple of adjacent pixels for two added lines, over the detection field. The Most Illuminated Pixel (MIP) defines the position of the first SATU centering window. The next step in the acquisition sequence is then initiated and consists of a centering phase where the SATU output signal is pre-processed for spot presence survey over the maximum of 10x10 pixel field. This allows the third phase to begin: the tracking phase.
The centering phase has occasionally resulted in loss of the star from the field of view. The fig. 3.2-1 reports the percentage of the stars lost in centering for the period 03-FEB-2003 to 02-NOV-2003. It can be seen that some stars, mainly weak stars (higher star id means higher magnitude) are lost during centering phase in more than 4% of their planned observations. As the monitoring shows neither trend nor excessively high percentages of loss, there is no need for the moment to reject any star from the catalogue, and there is no indication of instrument-related problems.

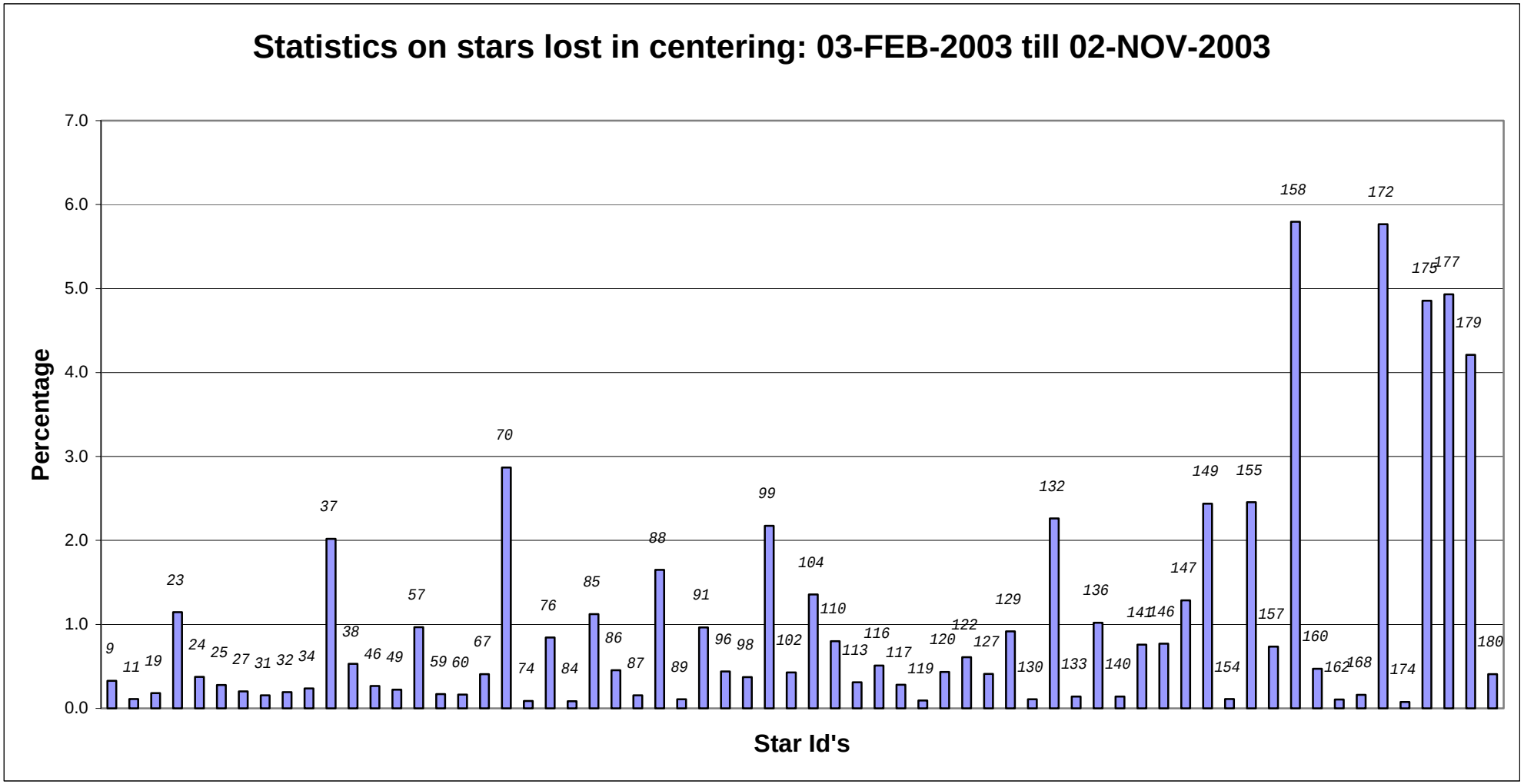

Figure 3.2-1: Statistics on stars that have been lost during the centering phase. The numbers above the columns correspond to the Star Id's.

3.3 Data generation gaps

The trend in percentage of available data within the archives PDHS-K and PDH-E is depicted in fig. 3.3-1 (when instrument was in operation). It is a good indicator on how the PDS chain is working in terms of generation and dissemination of data to the archives. The percentage is calculated once per week.

The availability of level 1b data within the archives is quite stable around 97% during the whole month of October. Also the level 0 availability is stable being the percentage situated almost at 99%.

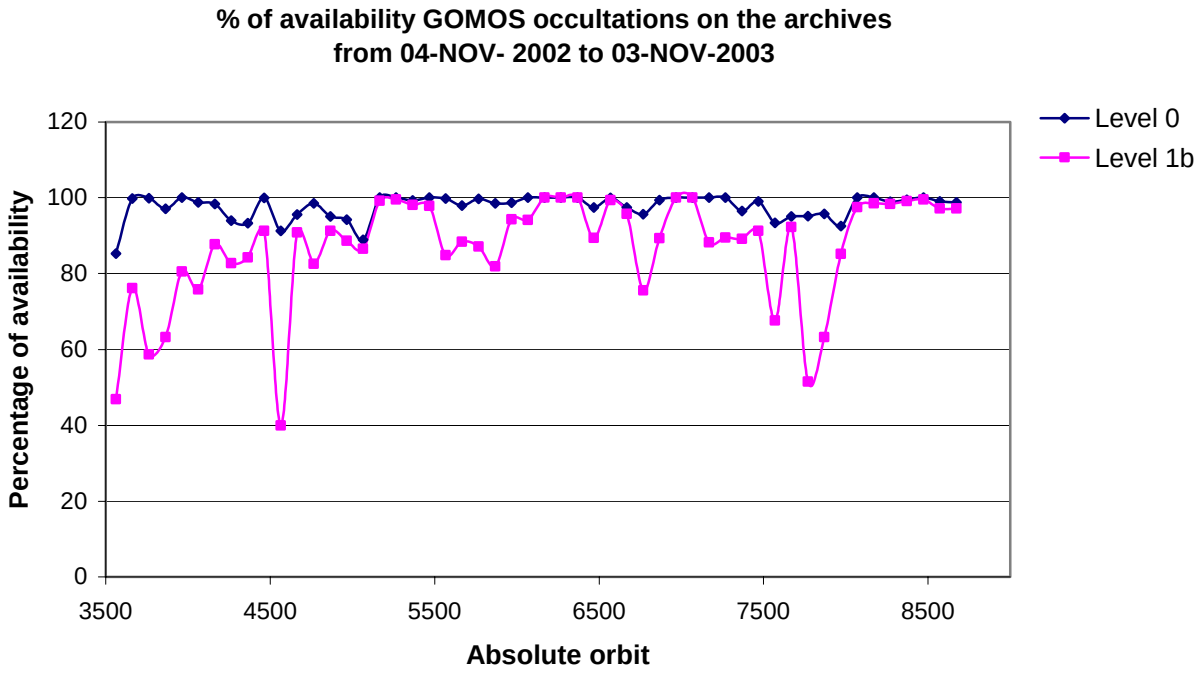

Figure 3.3-1: Percentage of level 0 and level 1b data availability on the archives PDHS-E and PDHS-K

3.3.1 GOM_NL__0P

Occultations planned to be acquired but for which no GOM_NL__0P data product has become available are presented in fig. 3.3-2 for the month of October 2003.

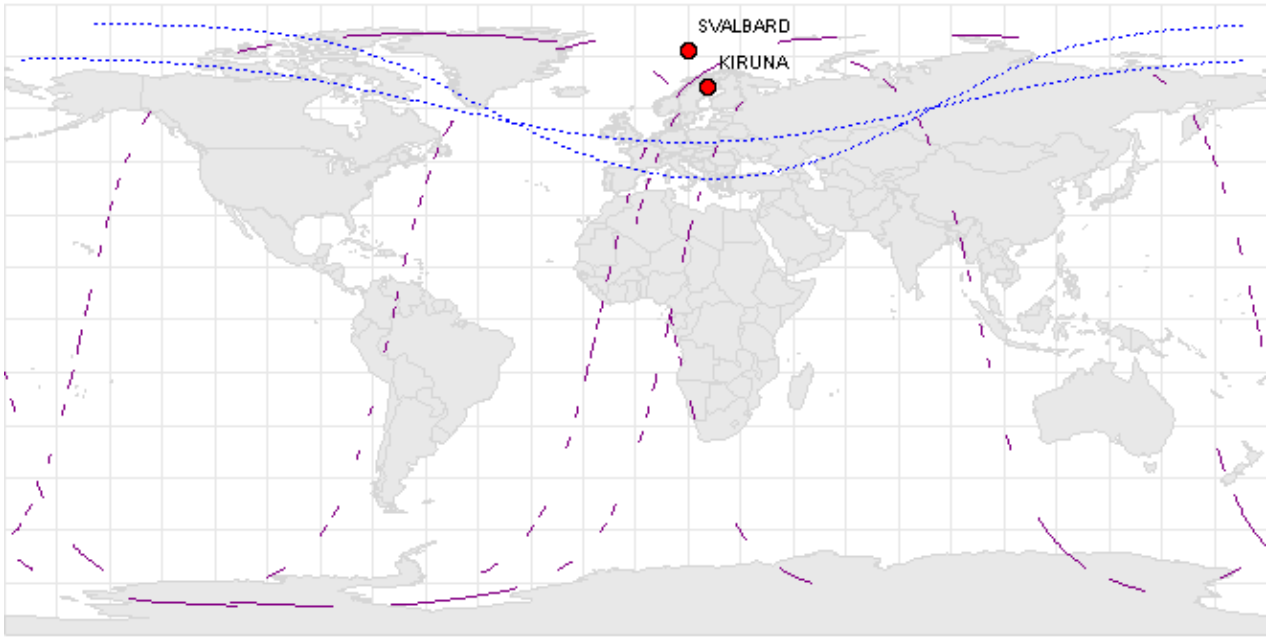

Figure 3.3-2: Orbit segments corresponding to planned data acquisitions for which no GOMOS level 0 product has become available

3.3.2 HIGHER-LEVEL PRODUCTS

Routine dissemination of higher-level products produced by the PDS to Cal/Val teams and other users is enabled. Currently ESA provides the Cal/Val teams with selected products that are generated with the prototype processor developed and operated by ACRI.

4 INSTRUMENT CONFIGURATION AND PERFORMANCE

4.1 Instrument Operation and Configuration

Since end of March the instrument has suffered some changes in the minimum azimuth range configuration in order to avoid the anomaly "Voice_coil_command_saturation" that caused the instrument to go into STAND BY/REFUSE mode. Since the change to the redundant chain B on July, the full range in azimuth has been again used (table 4.1-1).

Table 4.1-1: Historical changes in Azimuth configuration

Date	Orbit	Minimum Azimuth
29-MAR-2003 17:40	5635	0.0
31-MAY-2003 06:22	6530	+4.0
16-JUN-2003 16:17	6765	+12.0
15-JUL-2003 01:39	7200	-10.8

The operations of the instrument in other modes than occultation mode are identified in table 4.1-2.

There was no new Configurable Table Interface (CTI) uploaded to the instrument. The files used since the beginning of the mission are in table 4.1-3.

Table 4.1-2: GOMOS operations during October 2003

UTC time	Start orbit	Stop orbit	Mode (Asynchronous or Synchronous)	Calibration (CAL) or Dark Sky Area (DSA)
04 Oct 2003 06:56:58	8334	8341	A	CAL54
11 Oct 2003 06:36:51	8434	8434	A	DSA78
18 Oct 2003 06:16:44	8534	8534	A	DSA79
25 Oct 2003 05:56:37	8634	8634	A	DSA80

Table 4.1-3: Historic CTI files

CTI filename	Dissemination to FOCC
CTI_SMP_GMVIEC20030716_123904_00000000_00000004_20030715_000000_20781231_235959.N1	16-JUL-2003
CTI_SMP_GMVIEC20021104_075734_00000000_00000003_20021002_000000_20781231_235959.N1	06-NOV-2003
CTI_SMP_GMVIEC20021002_082339_00000000_00000002_20021002_000000_20781231_235959.N1	07-OCT-2003
CTI_SMP_GMVIEC20020207_154455_00000000_00000000_20020301_032709_20781231_235959.N1	21-FEB-2002

4.2 Thermal Performance

Since the beginning of the mission the hot pixel and RTS phenomena (see section 4.4.1) are producing a continuous increase of the dark charge signal within the CCD detectors. In order to minimize this effect, three successive CCD cool down were performed in orbits 800 (25th April 2002), 1050 (13th May 2002) and 2780 (11th September 2002) with a total decrease in temperature of 14 degrees.

Fig. 4.2-1 and 4.2-2 display, respectively, the overall temperature variation and the temperature variation around the Ascending Node Crossing (ANX) time with a resolution of 0.4 degrees (coding accuracy for level 0 data). The CCD temperatures during October are slightly higher than the ones registered in September. The expected seasonal variation of the temperatures with amplitude of around one degree can be clearly observed. The peaks that occur mainly in spectrometer B1 and B2 are also to be noted. They happen a little before the ANX for some consecutive orbits and every 8-10 days. Their origin is still not known, as we did not find any correlation between these peaks and other activities carried out on the satellite. The CCD temperature at almost the same latitude location (fig. 4.2-2) is monitored in order to detect any inter-orbital temperature variation.

The decrease observed on 24th March and twice in September in all detectors is after GOMOS switch off periods, when the instrument did not have enough time to reach the nominal temperature before starting the measurements.

The orbital temperature variation of the detector SPB2 (fig. 4.2-3 for & 4.2-4) is nominal being the maximum difference between ascending and descending passes around 2.4 degrees. The stability of the temperature during the orbit is important because it affects the position of the interference patterns. The phenomenon of the interference is present mainly in SPB and this Pixel Response Non-Uniformity (PRNU) is corrected during the processing.

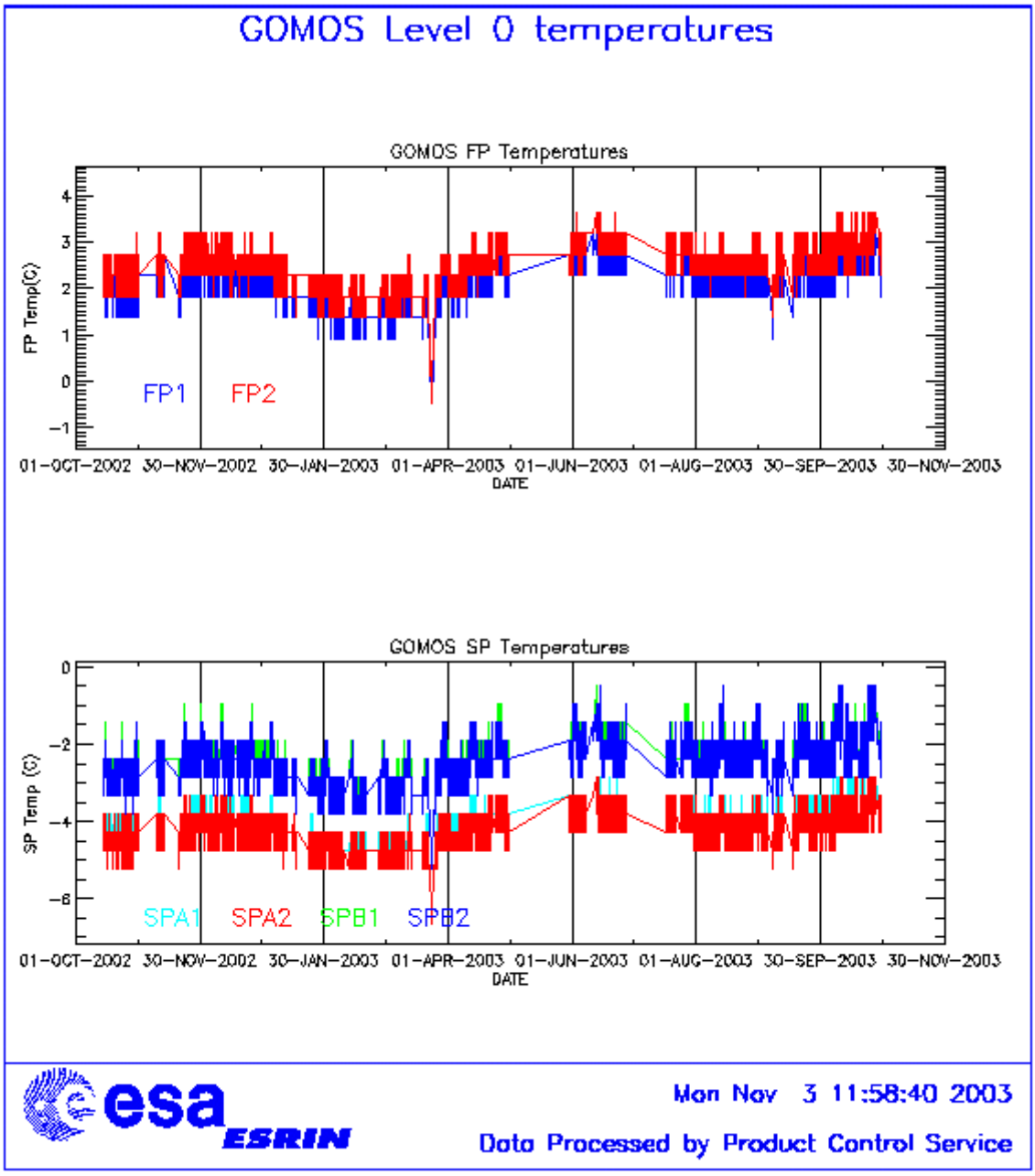

Figure 4.2-1: Level 0 temperature evolution of all GOMOS CCD detectors from October 2002 until end of October 2003

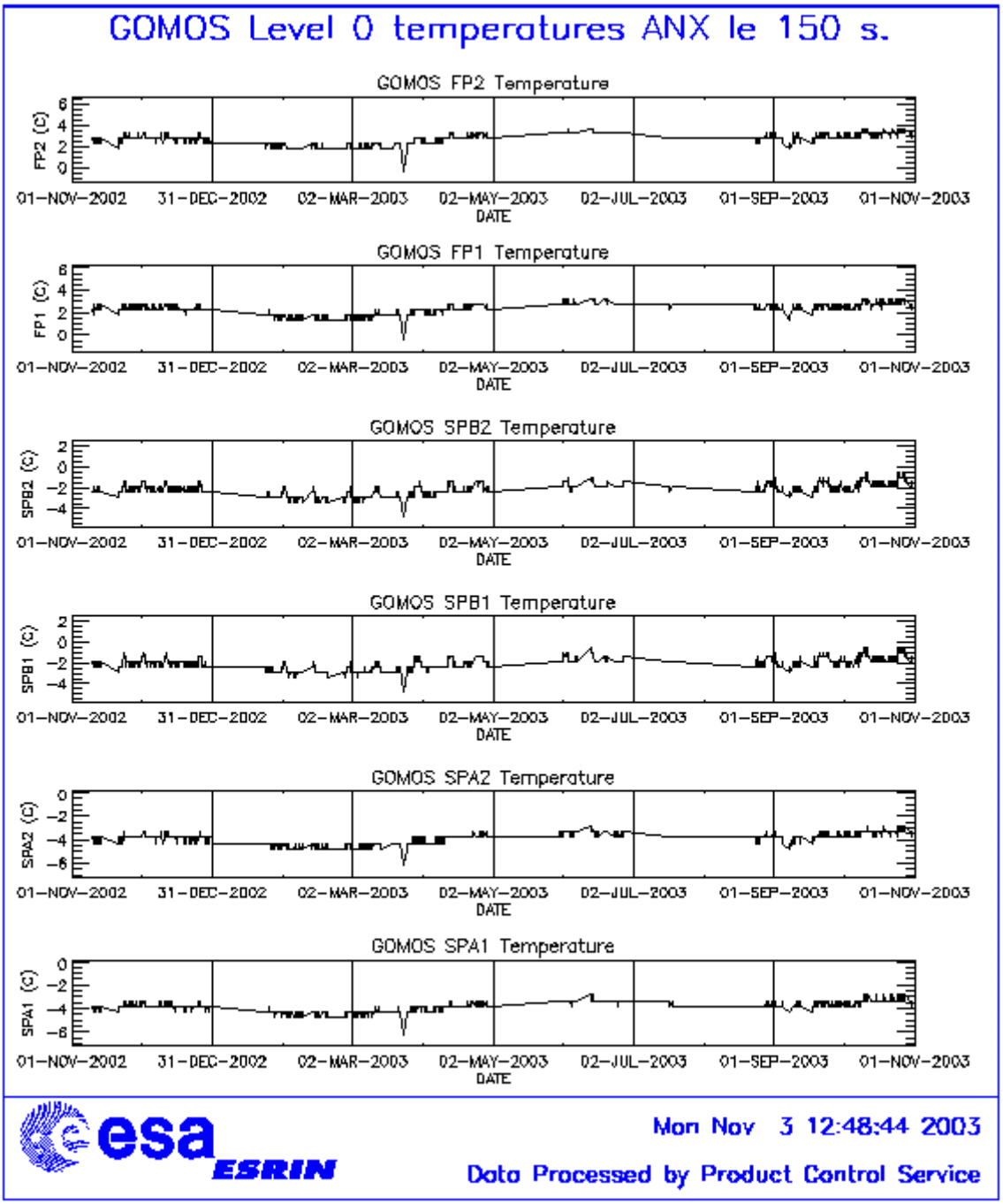

Figure 4.2-2: Level 0 temperature evolution of all GOMOS CCD detectors around ANX from November 2002 until end of October 2003

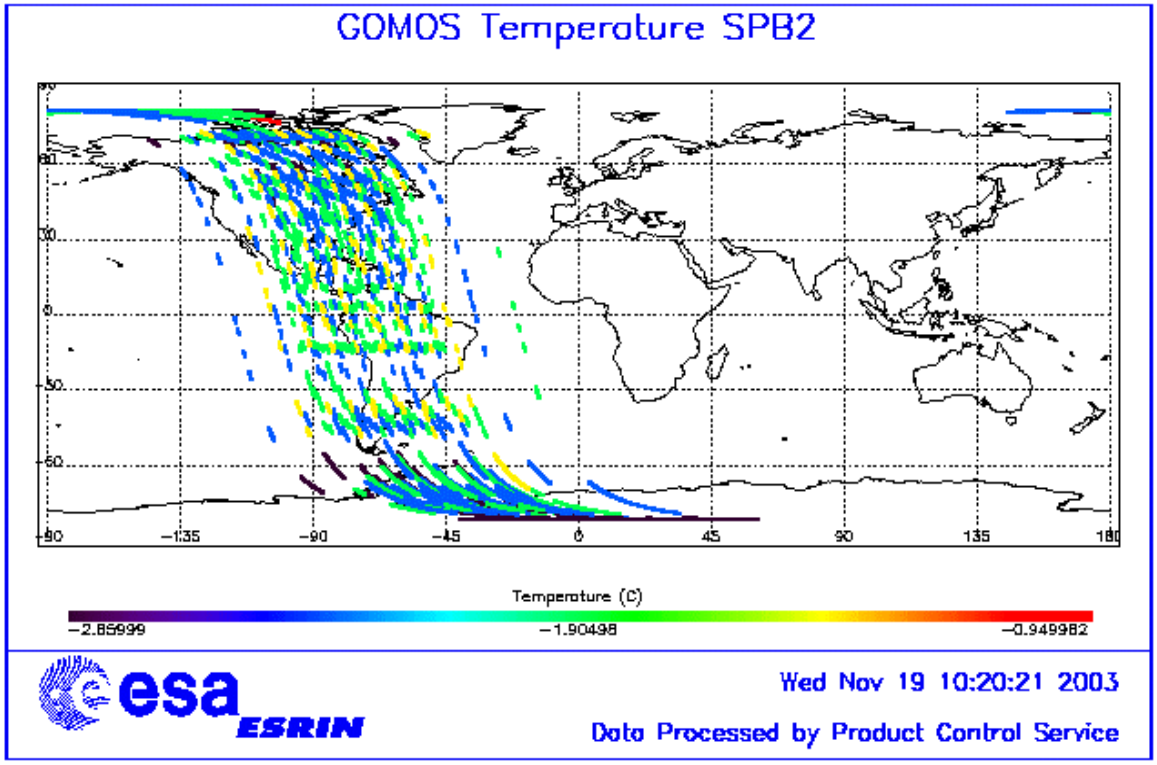

Figure 4.2-3: Ascending orbital variation of SPB2 temperature during some orbits on October 2003

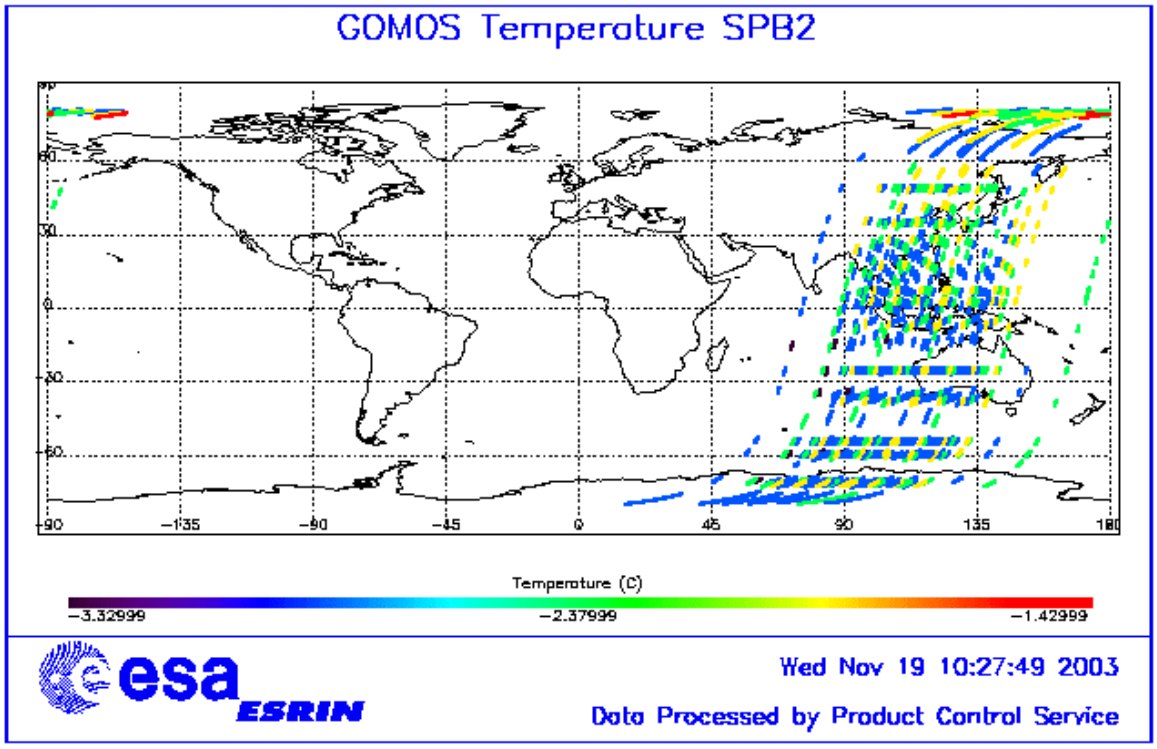

Figure 4.2-4: Descending orbital variation of SPB2 temperature during some orbits on October 2003

4.3 Optomechanical Performance

No new band setting calibration has been performed during October. These results were already presented in previous versions of the MR.

The position of stellar spectra of star id 2, 9 and 18 observed in dark-limb spatial spread monitoring mode have been averaged above 120 km altitude, and compared to the average positions before the transition to redundant chain on 15th July 2003 (blue dots in fig. 4-3.1). In table 4.3-1 the mean values of the location of the star signal for all the calibration analysis done till now are reported. The 'left' and 'right' values are calculated (the whole interval is not used) because the spectra present a slight slope, more pronounced in the spectrometer B (see fig. 4-3.1). The current processors GOMOS IPF 4.00 and GOPR prototype 5.4 still expect the spectra to be aligned along CCD lines, and therefore use only a single average line index per CCD. The values currently implemented of 81, 80, 82, 82 for SPA1, SPA2, SPB1 and SPB2 are still compatible with the observed 'left' and 'right' average position. The lookup table implemented in the version 6.0 of the prototype level 1 processor has been updated in order to have the line index as a function of the wavelength.
In table 4.3-2, mean values of the location of the star signal are calculated for some specific wavelength intervals. These intervals have been changed between the calibration performed in September 2002 and the ones performed afterwards. The results obtained are very similar to the ones obtained in previous exercises.
Table 4.3-3 reports the average location of the star spot on the photometer 1 and 2 CCD. No difference has been found for both photometers in column and in row positions.

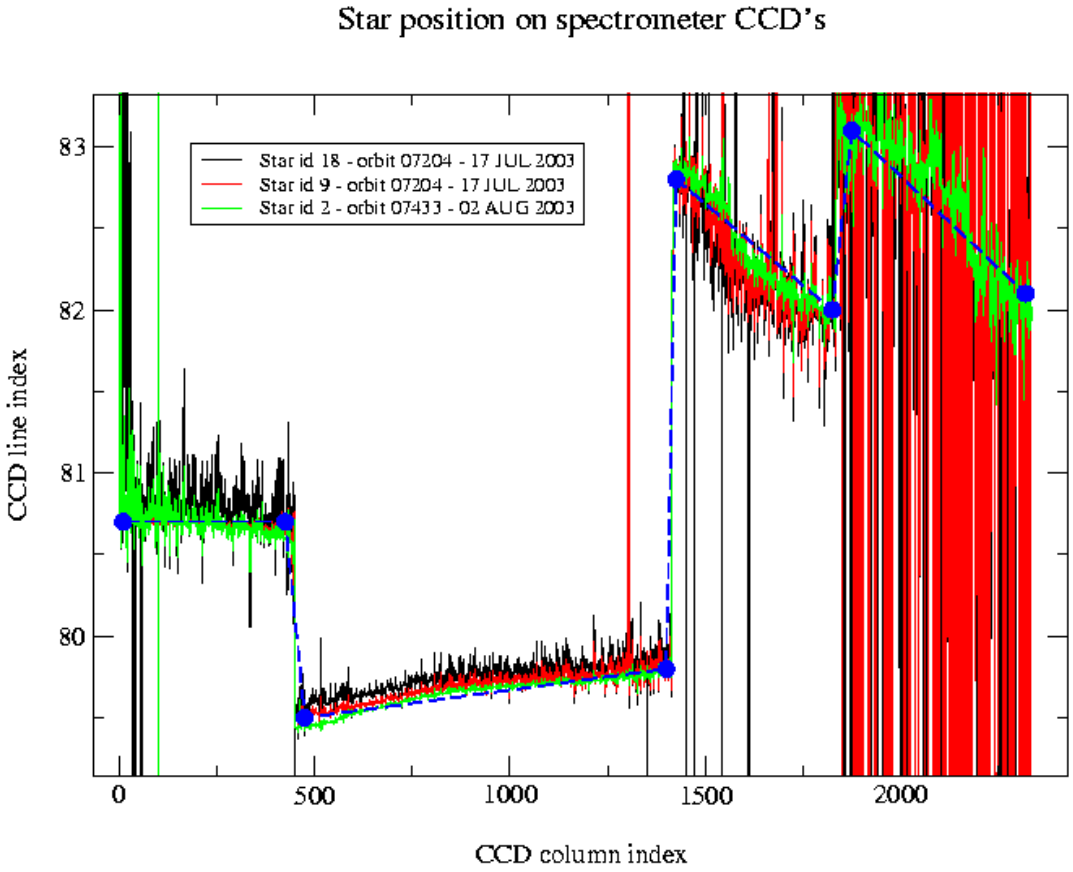

Figure 4.3-1: Average position of star spectra on the CCD

Table 4.3-1: Mean value of the location of the star signal during the occultation at the edges of every band (mean over 50 values, filtering the outliers)

	UV (SPA1) left/right	VIS (SPA2) left/right (Inverted spectra)	IR1 (SPB1) left/right	IR2 (SPB2) left/right
11/09/2002	80.7/80.7	79.8/79.5	82.8/81.9	83.1/82.1
01/01/2003	80.7/80.6	79.8/79.5	82.8/82.0	83.2/82.2
17/07/2003 & 02/08/2003	80.7/80.7	79.8/79.5	82.8/81.9	83.1/82.1

Table 4.3-2: Mean value of the location of the star signal during the occultation (as table 4.3-1) but now within some wavelength intervals

	UV (SPA1)	VIS (SPA2)	IR1 (SPB1)	IR2 (SPB2)
11/09/2002	80.8	79.8	82.6	82.9
wl range (nm)	[300-330]	[500-530]	[760-765]	[937-942]
01/01/2003	80.6	78.6	81.6	80.3
wl range (nm)	[350-360]	[650-670]	[760-765]	[935-945]
02/08/2003	80.6	79.7	82.5	82.8

Table 4.3-3: Average column and row pixel location of the star spot on the photometer CCD during the occultation

	FP1 (column/row)	FP2 (column/row)
11/09/2002	11/4	5/5
01/01/2003	10/4	6/4.9
02/08/2003	10/4	6/5

4.4 Electronic Performance

4.4.1 DARK CHARGE EVOLUTION AND TREND

The trend of Dark Charge (DC) is of crucial importance for the final quality of the products, and is therefore subject to intense monitoring. As part of the DC there is:

- "Hot pixels", a pixel is "hot" when its dark charge exceeds its value measured on ground, at the same temperature, by a significant amount.
- RTS phenomenon (Random Telegraphic Signal), it is an abrupt change (positive or negative) of the CCD pixel signal, random in time, affecting only the DC part of the signal and not the photon generated signal.

The temperature dependence of the DC would make this parameter a good indicator of the DC behaviour, but the hot pixels and the RTS are producing a continuous increase of the DC (see trend in fig. 4.4-1 and 4.4-2). To take into account these phenomena, in the last version of the level 1 processor (GOMOS/4.00) operational since May 2003, a DC map per orbit is extracted from a Dark Sky Area (DSA) observation performed around ANX (full dark conditions). For every level 1b product (occultation), the actual thermistor temperature of the CCD is used to convert the DC map measured around ANX into an estimate of the DC at the time (and different temperature) of the actual

occultation. When the DSA observation is not available, the DC map inside the calibration product that was measured at a given thermistor reference temperature is used; again, the actual thermistor temperature of the CCD is used to compute the actual map.

In fig. 4.4-1 and 4.4-2 it is plotted the average DC inserted by the processor into the level 1b data products for the spectrometers SPA1 and SPB1 (per band: upper, central and lower). From the figures, it can be noted that the rate of increase of DC for the last months is different from the first month's rate.

The same DC values are plotted in fig. 4.4-3 but for some occultations only during the reporting period.

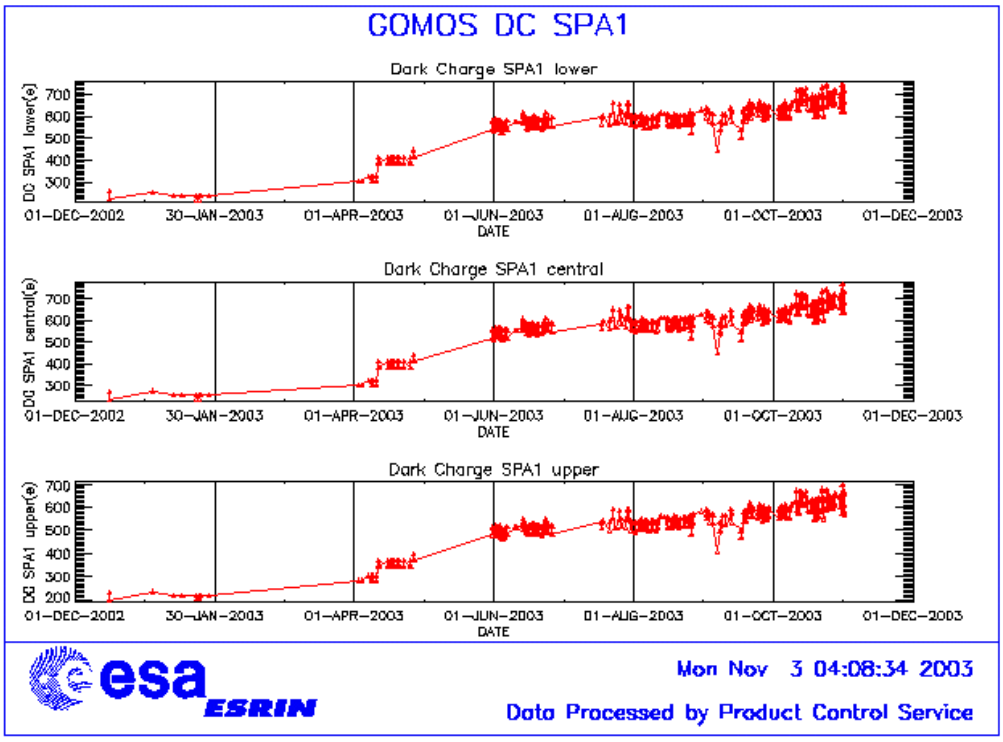

Figure 4.4-1: Mean DC evolution on SPA1 from 15th December 2002 until end of October 2003

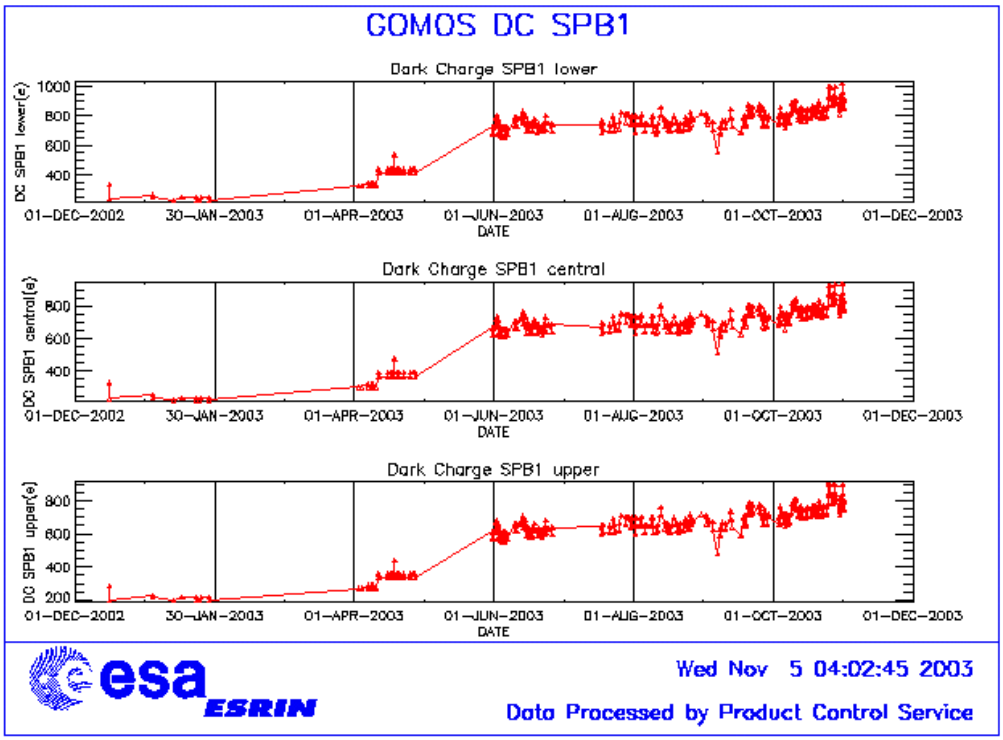

Figure 4.4-2: Mean DC evolution on SPB1 from 15th December 2002 until end of October 2003

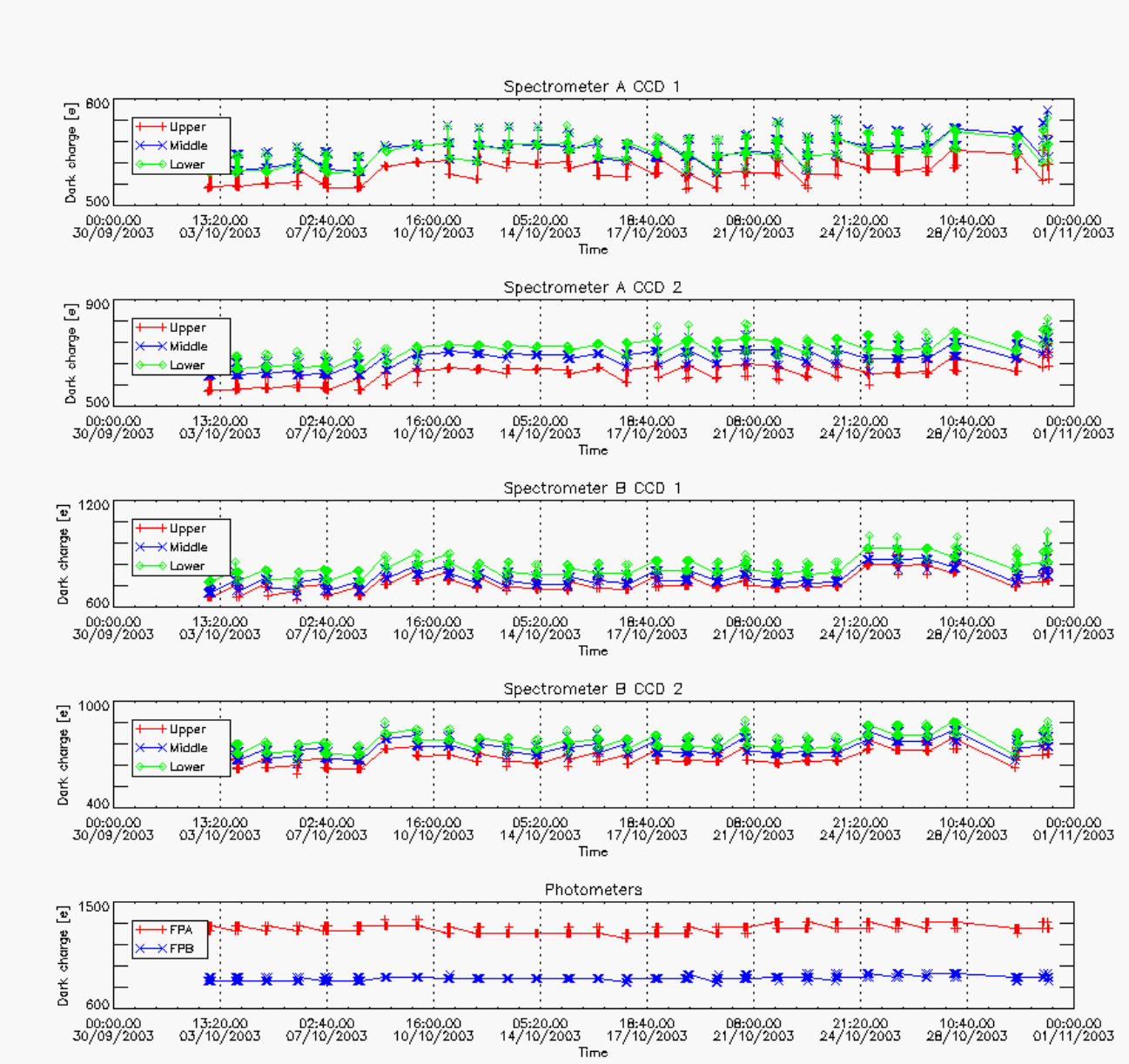

Figure 4.4-3: Mean Dark Charge of spectrometers and photometers during October 2003

4.4.2 SIGNAL MODULATION

A parasitic signal was found to be systematically present, added to the useful signal, at least for spectrometers A1 and A2. The modulation is corrected in the data processing, but the modulation signal standard deviation is routinely monitored in order to detect any trend (fig. 4.4-4).

The modulation standard deviation, for every spectrometer, is characterised as follows:

$$\sigma_{mod} = (\text{'static noises'} - \text{'total static variance'})^{1/2} / \text{gain} \qquad \text{(in ADU)}$$

- The 'static noises' are calculated from the DSA observation performed once per orbit
- The 'total static variance' is obtained from ADF data (electronic chain noise, quantisation noise).

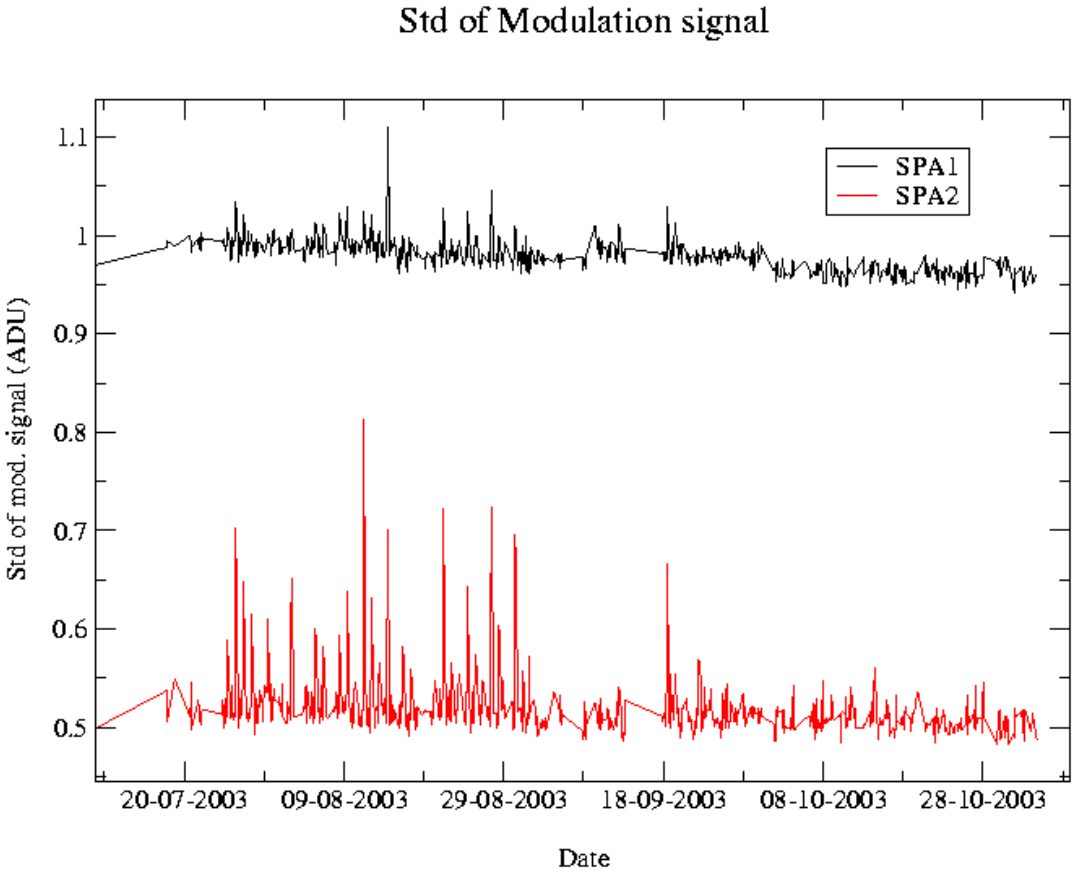

Figure 4.4-4: Standard deviation of the modulation signal

4.4.3 ELECTRONIC CHAIN GAIN AND OFFSET

No new electronic chain gain and offset calibration has been done during the reporting month so these results have been already presented in previous MR.

The routine monitoring of the ADC offset is a good indicator of the ageing of the instrument electronics. During the definition of this routine activity, an exercise has been done to analyse the variation of the ADC offset using the calibration observation in linearity mode (orbits 2810, 4384, 4834, 5219 and 5734).
The fig. 4.4-5 presents the evolution of the calibrated ADC offset for each spectrometer electronic chain. The unexpected increase of this offset seems to be due to an external contribution. In the ADC offset calibration procedure, linearity observations are used with two integration times of 0.25 and 0.50 seconds to extrapolate to an integration time of 0 seconds that give the complete chain offset and not only the ADC offset. The complete offset contains any possible offsets, and especially the static

dark charge (i.e. the dark charge that does not depend of the spectrometer integration time). If the memory area of the CCD is affected by the generation of hot pixels (this is confirmed by the presence of vertical lines visible in the measurement maps in spatial spread monitoring mode), it becomes that the increase observed in fig. 4.4-5 is due to these new hot pixels.

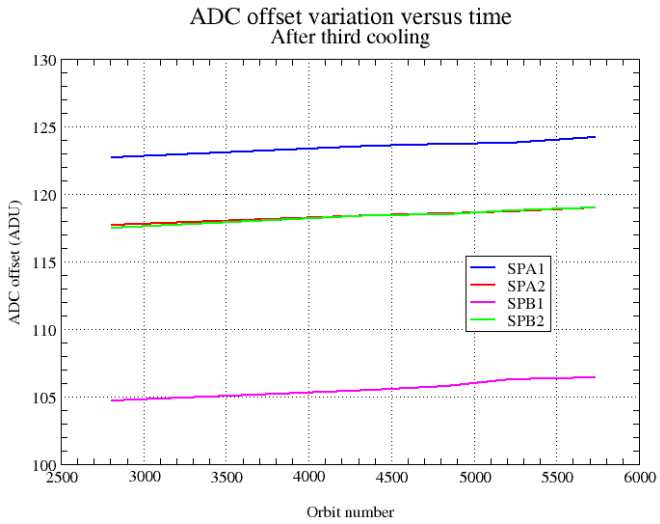

Figure 4.4-5: Evolution of the ADC offset for each spectrometer electronic chain

Next task consists in completing the analysis to confirm that the offset increase is due to the hot pixels in memory area. This can be proven by the study of the noise due to the increased dark charge. The increase of ADC offset will be assumed to be equal to the increase of 'static dark charge' and the corresponding noise will be computed and compared to the increase of the signal variance residual.

If we keep the ADC offset constant, as it is also used to compute the dark charge at band level used to correct the samples in the level 1b processing, the increase of the static dark charge - not taken into account in the ADC offset - is compensated by an artificial increase of the calibrated dark charge. So, the star and limb spectra are correctly corrected for dark charge. A small bias can be added to the instrument noise due to the incorrect dark charge level. Anyway, this quantity is not large enough to require a modification of the ADC offset value.

4.5 Acquisition, Detection and Pointing Performance

4.5.1 SATU NOISE AND EQUIVALENT ANGLE

The Star Acquisition and Tracking Unit (SATU) noise equivalent angle (SATU NEA) consists of the statistical angular variation of the SATU data above the atmosphere.
The mean of the standard deviation (std over the 50 values per measurement) above 105 km are computed for every occultation, giving two values per occultation: one in the 'X' direction, one in the 'Y' direction. A mean value per day in every direction is calculated and monitored in order to assess instrument performance in terms of star pointing. The thresholds are 2 and 3 micro radians in 'X' and 'Y' directions respectively. Before May 2003, data above 90 km have been considered (instead of 105

km) but from May 2003 on, data taken in the mesospheric oxygen layer (located around 100 km altitude) have been avoided because they could cause fluctuations on the SATU data. Also the products with errors (error flag set) are discarded from May 2003 onwards.
It can be seen in fig. 4-5.1 that the SATU NEA was stable and well below the thresholds during October.
The results for some occultations belonging to previous months (monthly averages) are presented in fig. 4.5-2, where no trend is visible so far.

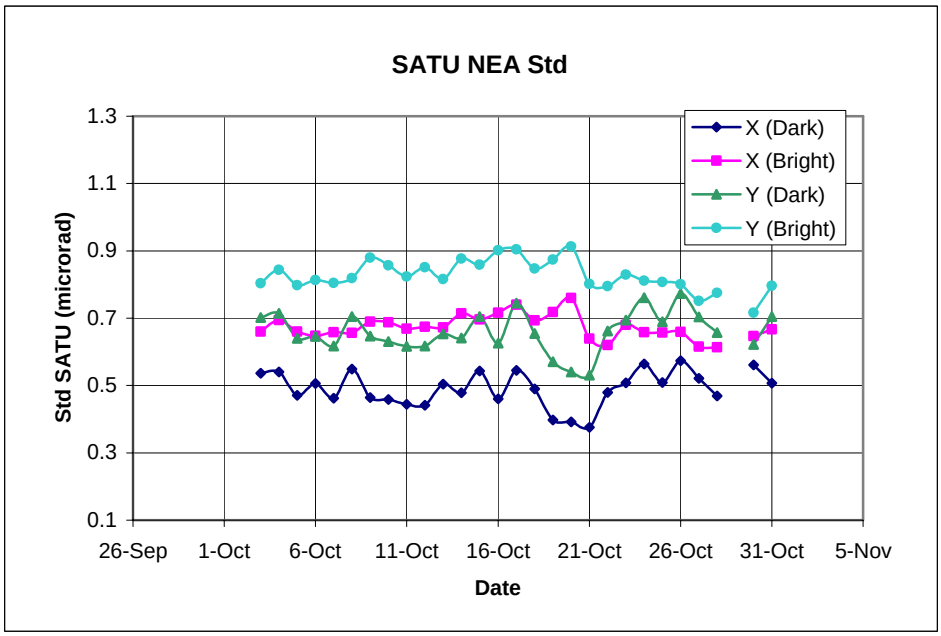

Figure 4.5-1: Average value per day of SATU NEA std above 105 kms

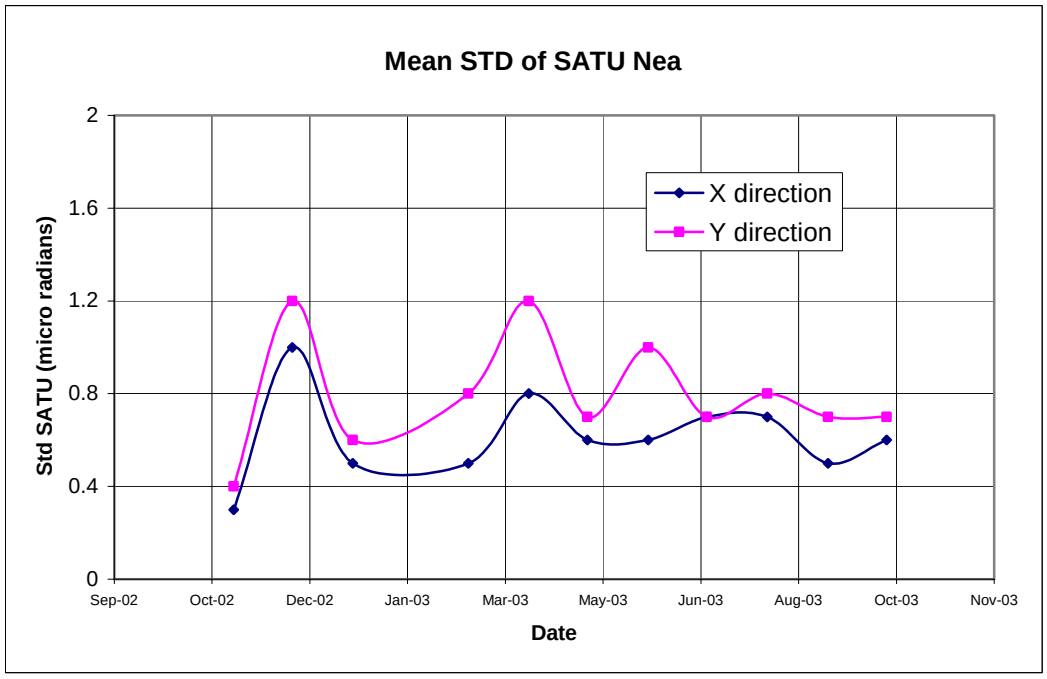

Figure 4.5-2: Average value per month of SATU NEA std above 105 kms

4.5.2 TRACKING LOSS INFORMATION

This verification consists of the monitoring of the tangent altitude at which the star is lost. It is an indicator of the pointing performance although it is to be considered that star tracking is also lost due to the presence of clouds and hence not only due to deficiencies in the pointing performance. Therefore, only the detection of any systematic long-term trend is the main purpose of this monitoring. The recent results are presented in fig. 4.5-3 and fig. 4.5-4:

- The dependence of the altitude at which tracking is lost on the magnitude of the star is very small because the tracking is mainly lost due to the refraction and the scintillation that depend on the atmospheric conditions.
- The majority of the stars lost at high altitude in fig. 4.5-3 belong to very long lasting occultations (very oblique ones) so it is not a fact related to deficiencies in pointing. There are two outliers in the same plot that belong to short occultations of the star id 52 on 14th and 16th October.
- In fig. 4.5-4 there are two occultations where the star is lost at high altitude and corresponds to star id 52.
- Some statistics are given in fig. 4.5-5 calculated for a set of data and not for the whole months. For the moment, no trend is visible in the plot.

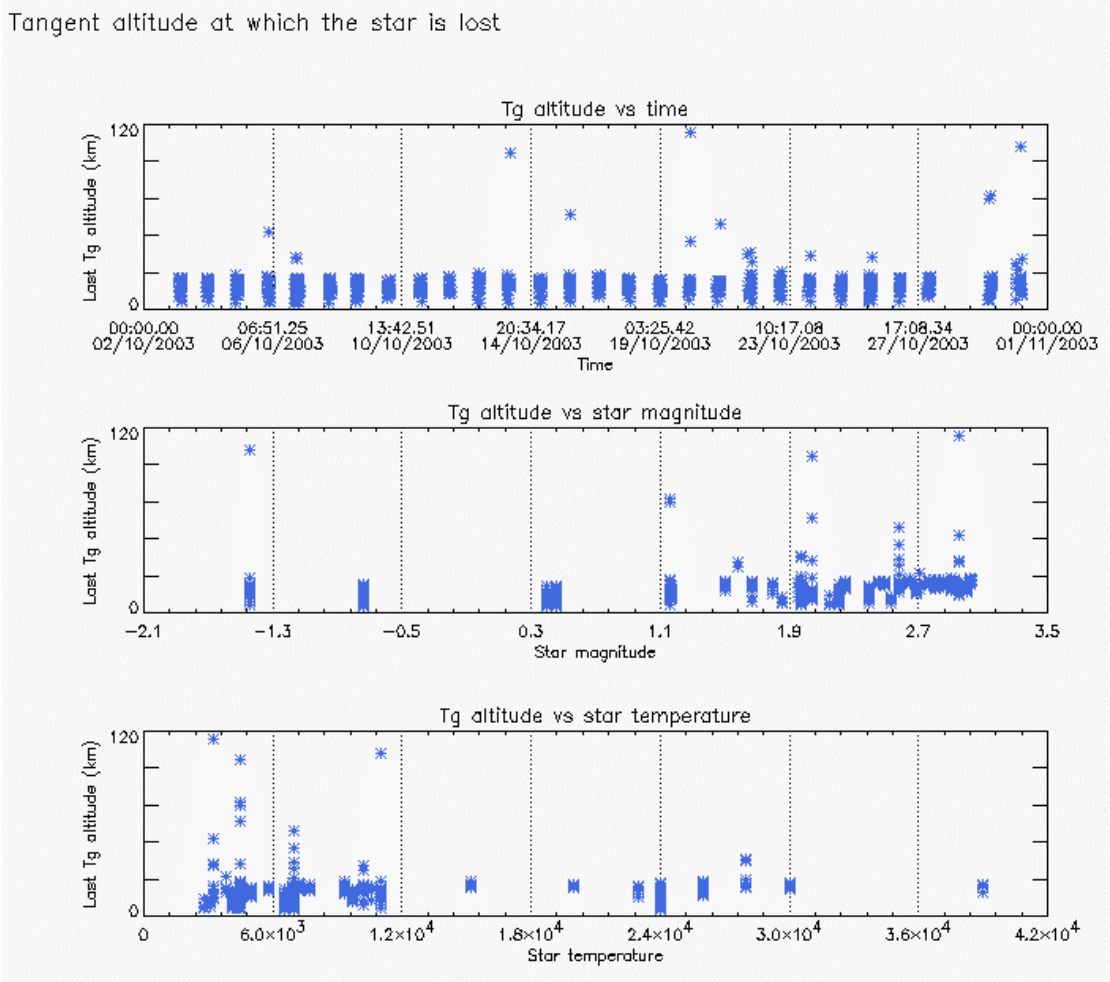

Figure 4.5-3: Last tangent altitude of the occultation (dark limb), point at which the star is lost

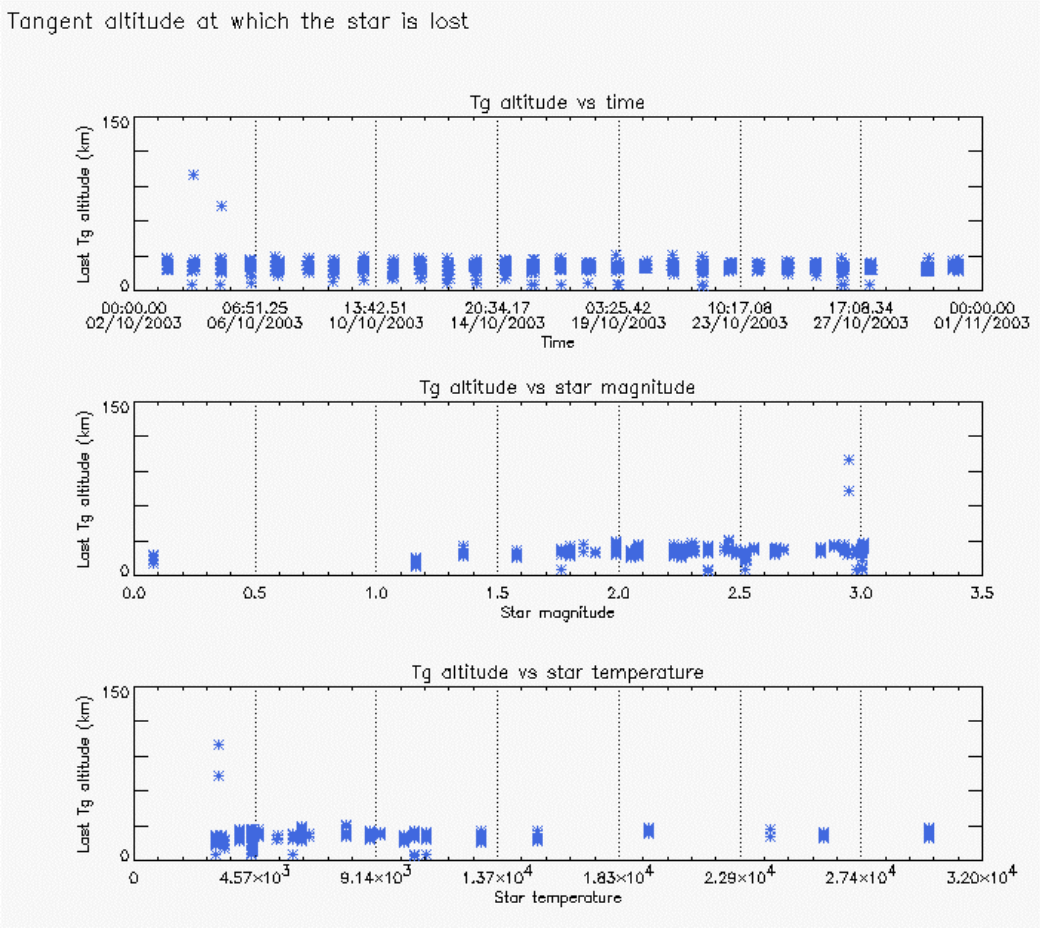

Figure 4.5-4: Last tangent altitude of the occultation (bright limb), point at which the star is lost

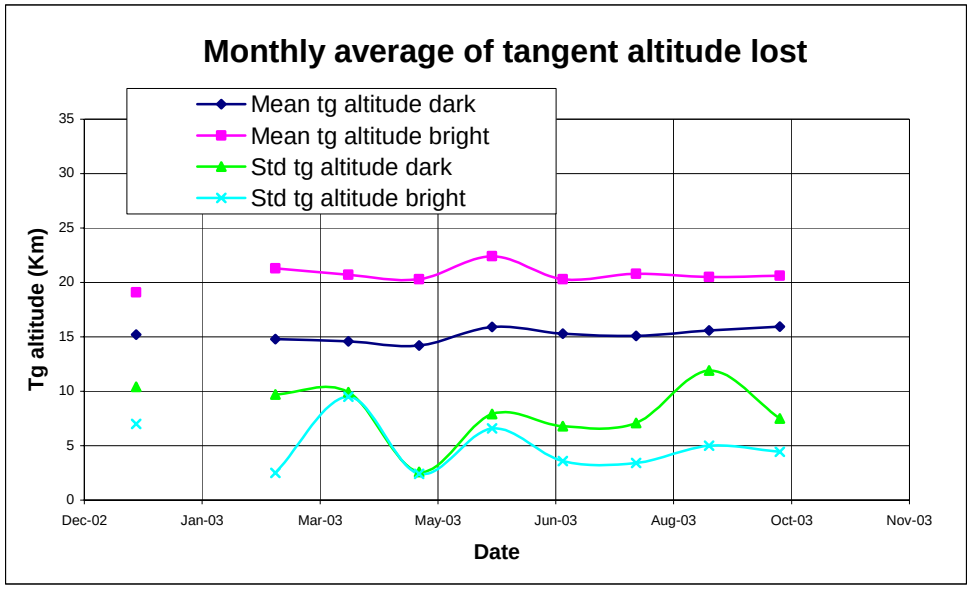

Figure 4.5-5: Mean tangent altitude (and Std) at which the star is lost for some occultations since January 2003

4.5.3 MIP (MOST ILLUMINATED PIXEL)

The MIP (Most Illuminated Pixel) is the star position on the SATU CCD in detection mode and it is recorded in the housekeeping data. The nominal centre of the SATU is pixel number **145** in elevation and number **205** in azimuth. The detection of the stars should not be far from this centre. As can be seen in fig. 4.5-6 the azimuth is always well within the threshold (table 4.5-1) since September 2002 even if a small variation is present. The elevation MIP has a significant variation and now the stars are detected 5 pixels above the SATU centre. The variation in MIP positions seems to be seasonal and it is an indicator of deviations from expected ENVISAT platform attitude. A mispointing of 0.1 degrees corresponds to a MIP variation onto the SATU CCD of 50 pixels. The MIP displacement will be carefully monitored. Fig. 4.5-7 shows the standard deviation of azimuth and elevation that should be within the thresholds of table 4.5-1. The peaks observed mean that one (or more) stars where detected very far from the SATU centre and, in this case, the star/s is lost during the centering phase (see section 3.2 for stars lost in centering).

Table 4.5-1: MIP thresholds

MIP X: mean delta Az	[198 - 210]
Std delta Az	7
MIP Y: mean delta El	[145 – 154]
Std delta El	4

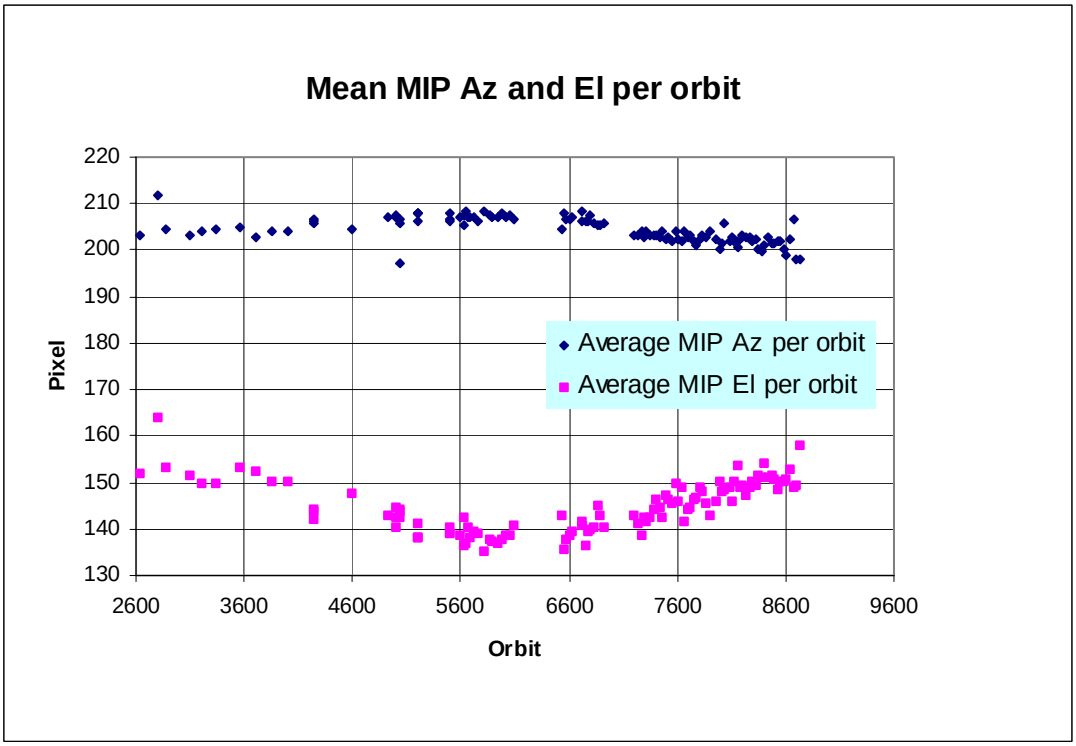

Figure 4.5-6: Mean values of MIP for some orbits since 1st September 2002 (see table 4.5-3)

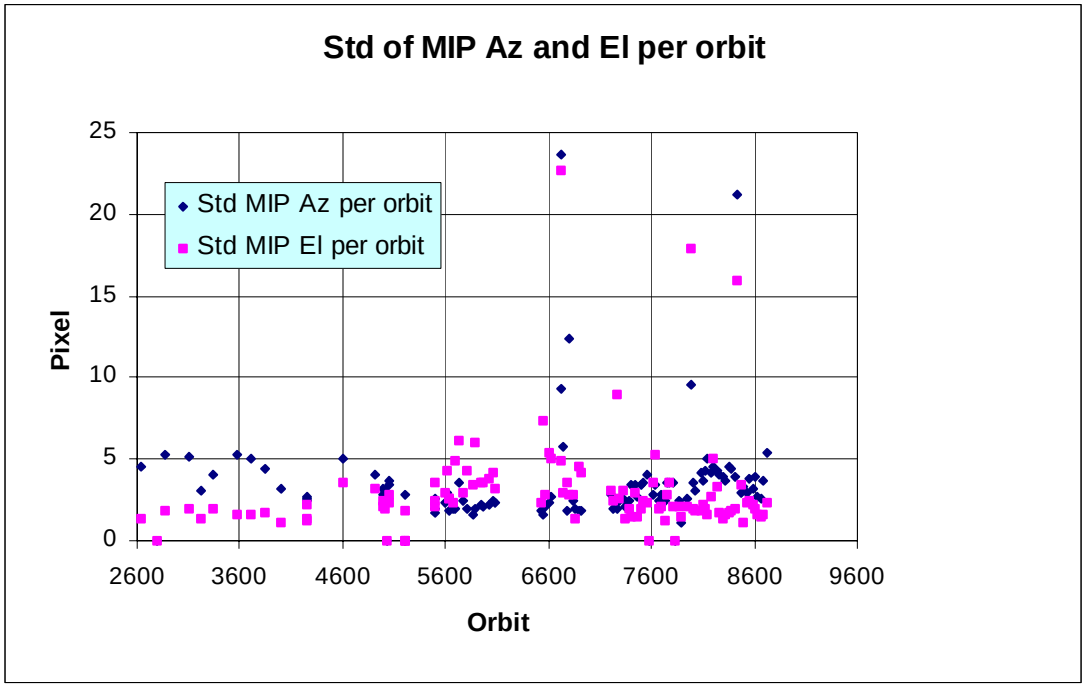

Figure 4.5-7: Standard deviation of MIP Azimuth and Elevation for some orbits since 1st September 2002 (see table 4.5-2)

5 LEVEL 1 PRODUCT QUALITY MONITORING

5.1 Processor Configuration

5.1.1 VERSION

About 12% of GOM_TRA_1P products have been received in the PCF for routine quality control and long term trend quality monitoring. The current level 1 processor software version for the operational ground segment is GOMOS/4.00 (see table 5.1-1) and the product specification is PO-RS-MDA-GS2009_10_3H. This processor has been cleared for initial level 1 data release, with a disclaimer for known artefacts that are currently being resolved and will be implemented in the next release (http://envisat.esa.int/dataproducts/availability).

Cal/Val teams are supplied with selected data sets generated by the prototype processor GOPR 5.4. See table 5.1-2 for the prototype level 1b versions and modifications.

Table 5.1-1: PDS level 1b product version and main modifications implemented

Date	Version	Description of changes
31-MAY-2003	Level 1b version 4.00 at PDHS-E and PDHS-K	Algorithm baseline level 1b DPM 5.4: • Modulation correction step added after the cosmic rays detection processing • Inversion of the non-linearity and offset corrections • Modification of the computation of the estimated background signal measured by the photometers: use the spectrometer radiometric sensitivity curve and the photometer transfer function. • Use of the dark charge map at orbit level computed from the DSA (dark sky area) if any in the level 0 product • Implementation of a new unfolding algorithm for the photometer samples • See ref. [2] for more details
21-NOV-2002	Level 1b version 3.61 at PDHS-E and PDHS-K	Algorithm baseline DPM 5.3: • Review of some default values • New definition of one PCD flag (atmosphere) • Temporal interpolation of ECMWF data • See ref. [2] for more details

Table 5.1-2: GOPR level 1b product version and main modifications implemented

Date	Version	Description of changes
25-JUL-2003	GOPR 5.4f	• The demodulation process is applied only in full dark limb and twilight limb conditions.
17-JUL-2003	GOPR 5.4e	• Sun zenith angle is computed in the geolocation process. The occultation is now classified into (0) full dark limb condition, (1) bright limb condition and (2) twilight limb condition. • No background correction applied in full dark limb condition. The location of the image of the star spectrum on the CCD array is no more aligned with the CCD lines.
02-JUL2003	GOPR 5.4d	• The maximum number of measurements is set to 509 (instead of 510) in the GOPR prototype.
17-MAR-2003	GOPR 5.4c	• Modification of the CAL ADFs (update of the limb radiometric LUT). The products are affected only if the limb spectra are converted into physical units • Modifications to allow compatibility with ACRI computational cluster (no modifications of the results) • Modification of the logic to handle dark charge map refresh at orbit level (DSA data is now directly processed by the level 1b processor if available in the level 0 product). No impact on the results
21-FEB-2003	GOPR 5.4b	• DC map values are rounded when written in the level 1b product • Modification of the CAL ADFs (update of the wavelength assignment of SPB1 and SPB2) • Modify the computation of flag_mod in the modulation correction routine
17-JAN-2003	GOPR 5.4a	• use the start and stop dates of the occultation when calling the CFI interpol instead of start and stop dates of the level 0 product • modify the ECMWF filename information in the SPH of the level 1b and limb products

5.1.2 AUXILIARY DATA FILES (ADF)

The ADF's files in tables 5.1-3 and 5.1-4 are used by the PDS to process the data from level 0 to level 1. For every type of file, the validity runs from the start validity time until the start validity time of the following one. The table 5.1-3 provides the whole set of auxiliary files used until now during the mission except for the calibration ADF files that are updated in a weekly basis. On 10th, 21st and 30th October new calibration ADF's were disseminated with updated DC map of orbits 08413, 08555 and 08695 respectively (table 5.1-4).

Table 5.1-3: Historic Level 1b ADF's

Filename	Validity time	Dissemination time
GOM_INS_AXVIEC20021112_170146_20020301_000000_20100101_000000	01-MAR-2002 → 16-JUL-2003	15-JUL-2003
GOM_INS_AXVIEC20030716_105425_20030716_120000_20100101_000000	16-JUL-2003	16-JUL-2003
GOM_PR1_AXNACR20021108_160000_20020301_000000_20100101_000000	01-MAR-2002 → 24-MAR-2002	08-NOV-2002
GOM_PR1_AXVIEC20030326_085805_20020324_200000_20100101_000000	24-MAR-2002	26-MAR-2003
GOM_STS_AXVIEC20020121_165822_20020101_000000_20200101_000000	01-JAN-2002	21-JAN-2002
GOM_CAT_AXIEC20020121_161009_20020101_000000_20200101_000000	01-MAR-2002	21-JAN-2002

Table 5.1-4: Calibration ADF for October 2003. These files are updated in a weekly basis

Filename	Validity time	Dissemination time
GOM_CAL_AXVIEC20031030_133050_20031027_000000_20100101_000000	27-OCT-2003	30-OCT-2003
GOM_CAL_AXVIEC20031021_101419_20031017_000000_20100101_000000	17-OCT-2003 → 26-OCT-2003	21-OCT-2003
GOM_CAL_AXVIEC20031010_124929_20031007_000000_20100101_000000	07-OCT-2003 → 16-OCT-2003	10-OCT-2003

5.2 Quality Flags monitoring

In this section it is monitored some Product Quality information stored in the level 1b products that are not flagged (MPH error flag not set). On the one hand, for every product we have information of the **number of measurements** where a given problem was detected (i.e. number of invalid measurements, number of measurements containing saturated samples, number of measurements with demodulation flag set…). On the other hand, there are **flags** that indicate problems within the product (i.e. flag set to one if the reference spectrum was computed from DB, flag set to zero if SATU data were not used…).

For the information on the number of measurements a plot (percentages) is provided in fig. 5.2-1. It can be seen that the cosmic rays hits occurred often for the 95% of the measurements of the product. Another observation that can be done is that, for many products, the 30 % of the measurements have the star signal falling outside the central band. The other values (% of invalid measurements per product, % of measurements per product with datation errors…) are quite low.

The flag information is given in table 5.2-1. It is reported also the percentage of the products that have at least one measurement with demodulation flag set.

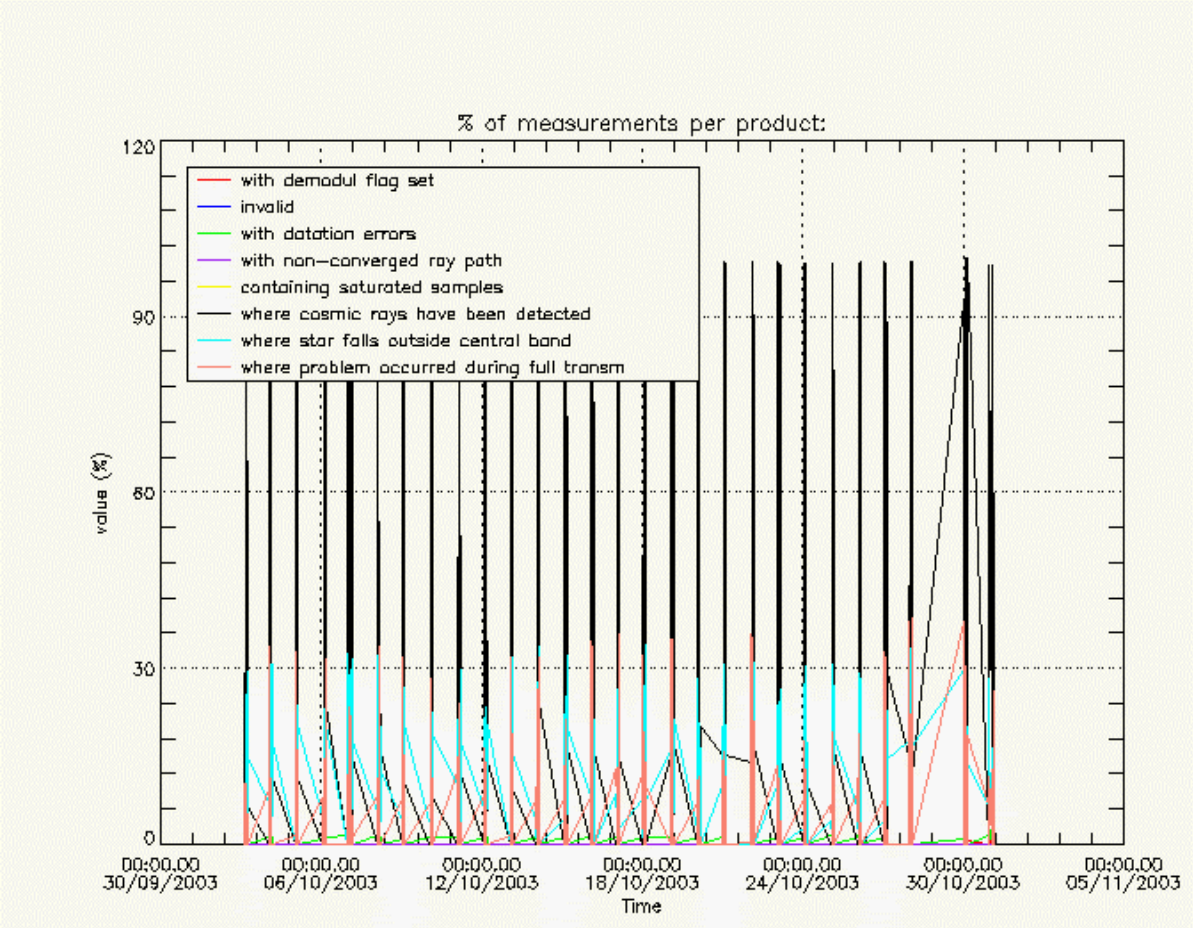

Figure 5.2-1: Level 1b product quality monitoring

Table 5.2-1: Percentage of products during the reporting period with:

At least one measurement with demodulation flag set:	17.4189 %
Reference spectrum computed from DB:	0.00000 %
Reference spectrum with small number of measurements:	0.00000 %
SATU data not used:	0.00000 %

5.3 Spectral Performance

No new spectral calibration has been done during October. These results were already presented in previous versions of the MR with nominal results thus far.

The values reported (table 5.3-1) are, for every star ID (1, 2, 4, 9, 18, 25), the wavelength of the first useful pixel of SPA2. This value is calculated by addition to the actual wavelength assignment, the spectral shift for which a maximum correlation has been found between the reference spectrum and the one of the occultation. It can be observed in table 5.3-1 that for all the stars (but for star id 4) the difference between the actual wavelength (690.492981 nm) and the one reported in the table is between –0.06 and 0.05 nm. Thus, the wavelength has not been updated in the Calibration product. It is foreseen not to use the star id 4 for wavelength calibration purposes.

Table 5.3-1: New wavelength assignment calculated for several occultations since November 2002.

Star ID / Level 0 date	1	2	4	9	18	25
20021112_062935	Occ.30: 690.455750	Occ.26: 690.458740		Occ.28: 690.492981		
20021219_102754		Occ.33: 690.468140	Occ.26: 690.875122			
20030101_151630	Occ.3: 690.445068	Occ.37: 690.466003	Occ.30: 690.878540			
20030110_121504		Occ.32: 690.465088	Occ.25: 690.882385			
20030201_090221						Occ.21: 690.492981
20030415_123156			Occ.29: 690.959534		Occ.20: 690.552002	Occ.28: 690.492981
20030419_170041			Occ.29: 690.957520		Occ.23: 690.555420	
20030428_072600					Occ.19: 690.553645	Occ.28: 690. 492981
20030717_053233				Occ. 22: 690.473816	Occ. 26: 690.446594	

5.4 Radiometric Performance

5.4.1 RADIOMETRIC SENSITIVITY

The monitoring performed consists in the calculation of the radiometric sensitivity of each CCD by computing the ratio between parts of the reference spectrum using specific stars. The parts of spectrum used are:

- UV: 250–300 nm
- Yellow: 500–550 nm
- Red: 640–690 nm
- Ir1: 761-770 nm
- Ir2: 935-944 nm

For the spectrometers the ratios are with respect to the ‘yellow’ spectral range. For the photometers, the ratio is calculated dividing the mean photometer signal above the atmosphere (115 km) by the ‘yellow’ spectral range (for PH1) or by the ‘red’ spectral range (for PH2).
In the plot (fig. 5.4-1) the ratios are normalized. The variation of the ratio should be within a given threshold actually set to 10% (see table 5.4-1). For every star, this variation is calculated as the difference between the maximum (or minimum) ratio, and the mean over the 15 first values (if there are not 15 values computed yet, all values are used). Values outside the warning threshold of 10% are now observed for the photometers, and investigation results will be reported in future monthly reports.

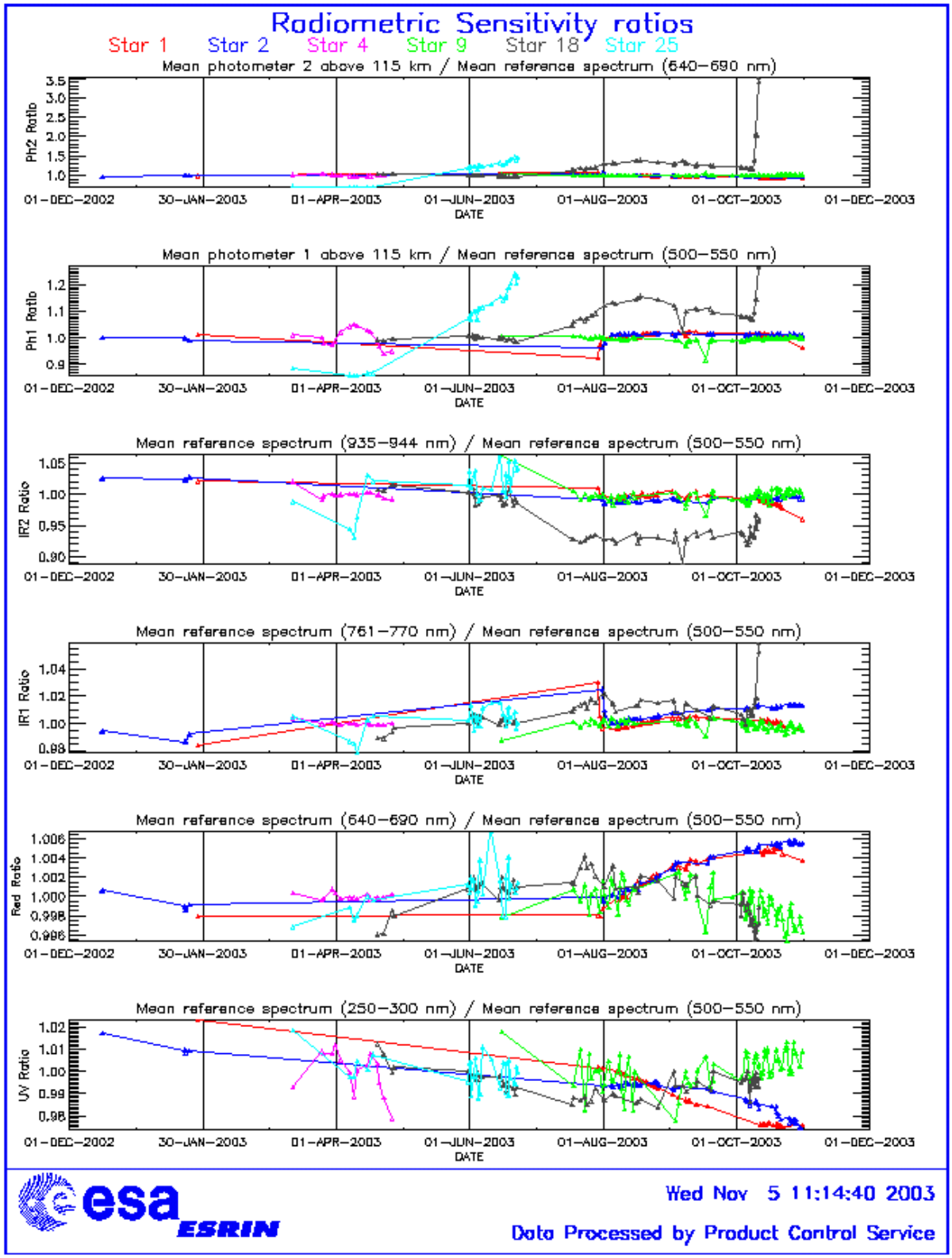

Figure 5.4-1: Radiometric Sensitivity ratios.

Table 5.4-1: Variation of RS for the different ratios. Should be less than 10%.

Star Id	% variation of UV ratio	% variation of Red ratio	% variation of IR1 ratio	% variation of IR2 ratio	% variation of Ph1 ratio	% variation of Ph2 ratio
1	0.543863	0.180867	0.387800	0.184993	4.16760	10.4636
2	0.139495	0.244293	0.418974	0.180858	2.10667	6.07233
4	0.0529779	0.0468850	0.115433	0.233174	2.51800	4.93374
9	1.65465	0.154361	0.142307	0.233455	4.79555	6.18962
18	0.223948	0.167108	0.844914	0.608099	14.7885	299.989
25	2.55773	0.212821	0.225987	0.223921	15.9214	78.6219

5.4.2 PIXEL RESPONSE NON UNIFORMITY (PRNU)

No new PRNU calibration has been done during October. During May a new PRNU calibration has been performed and processed into an update of the PRNU maps for the SPB1 and SPB2 that have been included in the auxiliary file GOM_CAL disseminated at the end of June 2003.

5.5 Other Calibration Results

Future reports will address other calibration results, when available.

6 LEVEL 2 PRODUCT QUALITY MONITORING

6.1 Processor Configuration

6.1.1 VERSION

No level 2 products from the operational ground segment have been disseminated during October to the users. About 80% of GOM_NL__2P products have been received in the PCF for routine quality control and long term trend monitoring. The current level 2-processor software version for the operational ground segment is GOMOS/4.00 (see table 6.1-1) and the product specification is PO-RS-MDA-GS2009_10_3H. The improvements defined at the Validation Workshop are currently being implemented into the prototype processor, before implementation into the operational one. In the mean time, Cal/Val teams are supplied with selected data sets generated by the previous prototype processor GOPR 5.4 (see table 6.1-2).

Table 6.1-1: PDS level 2 product version and main modifications implemented

Date	Version	Description of changes
31-MAY-2003	Level 2 version 4.00 at PDHS-E and PDHS-K	Algorithm baseline level 2 DPM 5.4: • Revision of some default values • Add a new parameter • Transmission model computation: suppress tests on valid pixels and species • Apply a Gaussian filter to the vertical inversion matrix • Very low signal values are substituted by threshold value • See ref. [3] for more details
21-NOV-2002	Level 2 version 3.61 at PDHS-E and PDHS-K	Algorithm baseline level 2 DPM 5.3a: • Revision of some default values • Wording of test T11 • Dilution term computation of jend • Covariance computation scaling applied before and after • See ref. [3] for more details

Table 6.1-2: GOPR level 2 product version and main modifications implemented

Date	Version	Description of changes
18-AUG-2003	GOPR 5.4d	• Tikhonov regularisation is implemented
18-MAR-2003	GOPR 5.4b	• Modification to implement the computation of Tmodel for spectrometer B (in version 5.4b, the Tmodel for SPB is still set to 1)
30-JAN-2003	GOPR 5.4a	• Modifications for ACRI internal use only. No impact on level 2 products.

6.1.2 AUXILIARY DATA FILES (ADF)

The ADF's files in table 6.1-3 are used by the PDS to process the data from level 1 to level 2. For every type of file, the validity runs from the start validity time until the start validity time of the following one.

Table 6.1-3: Historic Level 2 ADF's

Filename	Validity time
GOM_INS_AXVIEC20021112_170146_20020301_000000_20100101_000000	01-MAR-2002
GOM_PR2_AXVIEC20021112_170458_20020301_000000_20100101_000000	01-MAR-2002
GOM_CRS_AXVIEC20020729_082931_20020301_000000_20100101_000000	01-MAR-2002

6.2 Other Level 2 performance issues

The plot presented in fig. 6.2-1 is the average of the Ozone values during October in a grid of 0.5 degrees in latitude per 1 km in altitude. Some characteristics can be seen: part of the ozone hole beyond –60 degrees latitude; the increase of ozone layer thickness at around 20-25 km at high latitudes

due to the transport of O_3 rich air masses. However, other characteristics seem not to be realistic (and are under investigation) as the high values of ozone observed in the lower stratosphere.

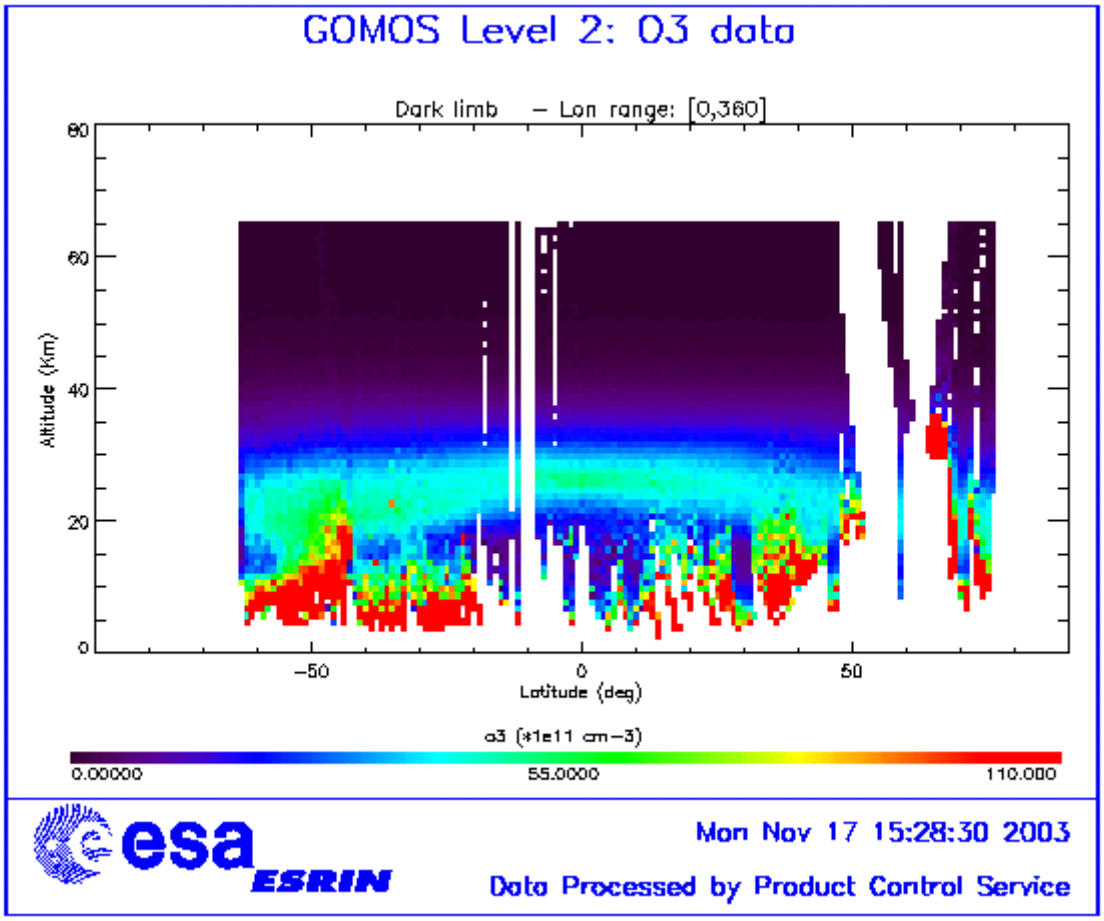

Figure 6.2-1: Average GOMOS O_3 profile during October: average in a grid of 0.5° latitude x 1 Km altitude

7 VALIDATION ACTIVITIES AND RESULTS

7.1 Intercomparison with external data

Results will be presented upon availability.

7.2 GOMOS-Climatology comparisons

Results will be presented upon availability.

7.3 GOMOS Assimilation

Results will be presented upon availability.

7.4 Consistency Verification: GOMOS-GOMOS intercomparison

Fig. 7.4-1, 7.4-2, 7.4-3, 7.4-4, 7.4-5, 7.4-6 illustrate the correlation between values of GOMOS air density and values of ECMWF air density, for altitudes between 25km and 35km. Results are presented for measurements in September 2002, in April 2003, and for the whole validation dataset (several months in 2002-2003), from profiles produced with both versions of level 2 (L2) processing, GOPR v5.4b and v5.4d.
Values of the correlation coefficient and of the standard deviation of the difference to the linear fit according to the L2 processing versions are summarized table 7.4-1. For the three periods of time, the correlation coefficient is higher and the standard deviation is lower when calculated with the L2 version v5.4d than with the version v5.4b.

Table 7.4-1: Correlation coefficient and standard deviation between GOMOS and ECMWF air density profiles for two different versions of the level 2 processing

	Correlation coefficient		Standard deviation	
	GOPR v5.4b	*GOPR v5.4d*	*GOPR v5.4b*	*GOPRv5.4d*
September 2002 (1057 L2 profiles)	0.78	**0.97**	0.15	**0.05**
April 2003 (438 L2 profiles)	0.75	**0.91**	0.16	**0.08**
2002-2003 (2326 L2 profiles)	0.73	**0.94**	0.17	**0.06**

Note: the major difference between L2 processing version v5.4b and v5.4d is the implementation of Tikhonov regularisation in the version v5.4d, besides other updates of L1b processing.

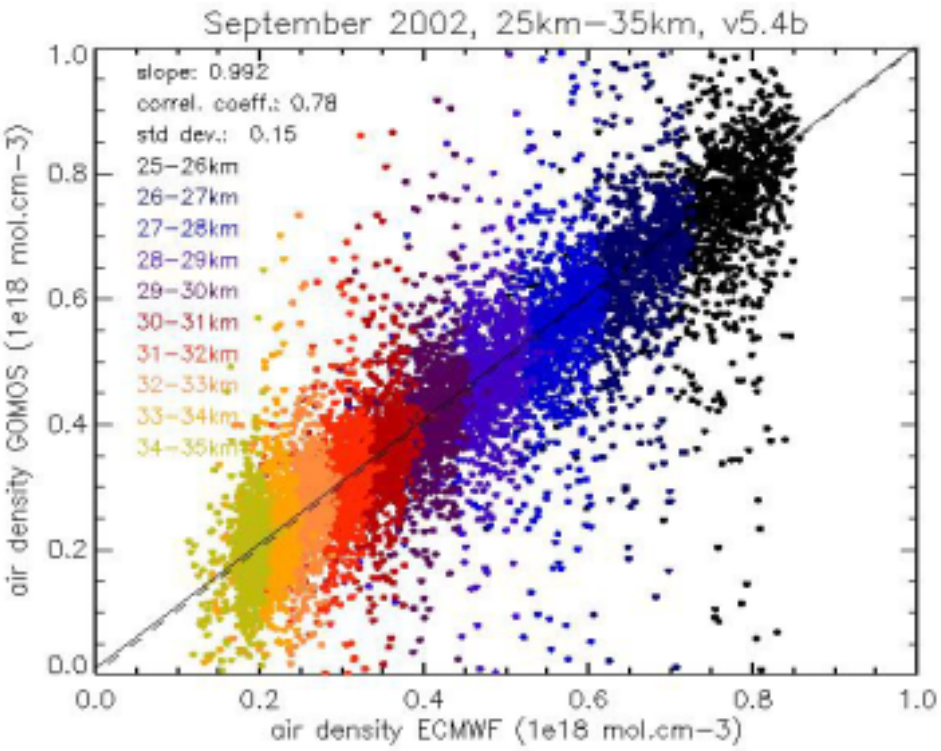

Figure 7.4-1: GOMOS air density vs ECMWF air density, September 2002, GOPR v5.4b

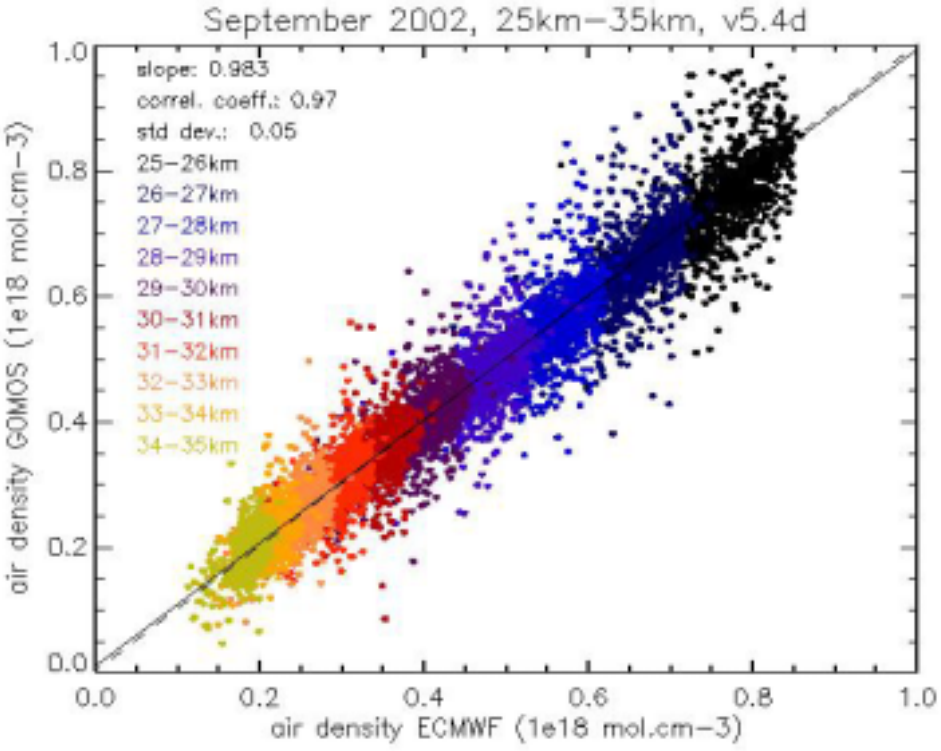

Figure 7.4-2: GOMOS air density vs ECMWF air density, September 2002, GOPR v5.4d

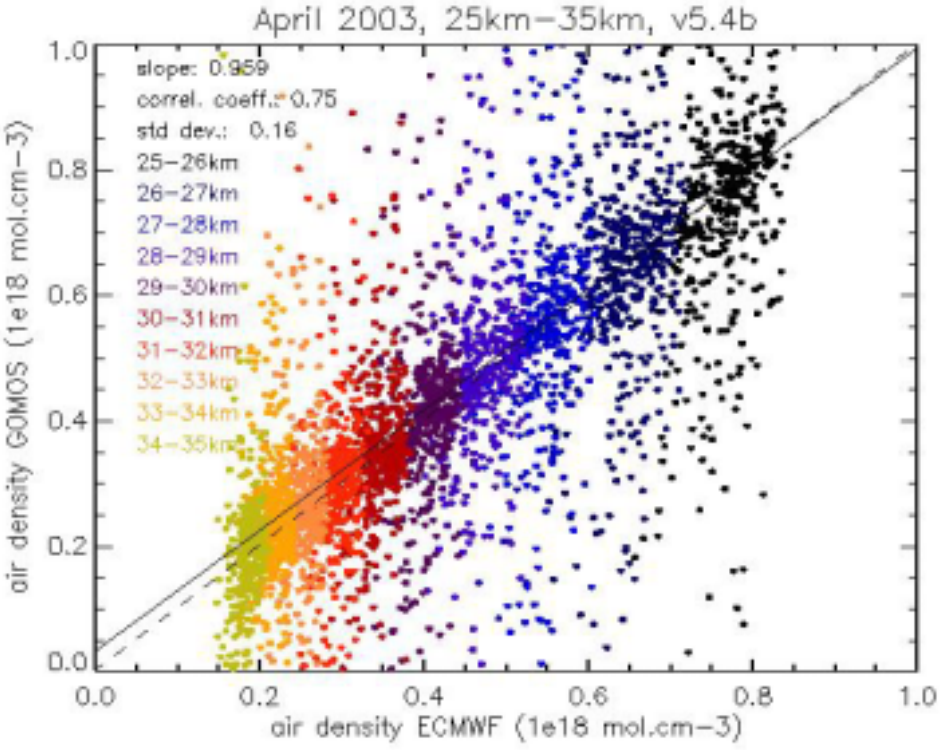

Figure 7.4-3: GOMOS air density vs ECMWF air density, April 2003, GOPR v5.4b

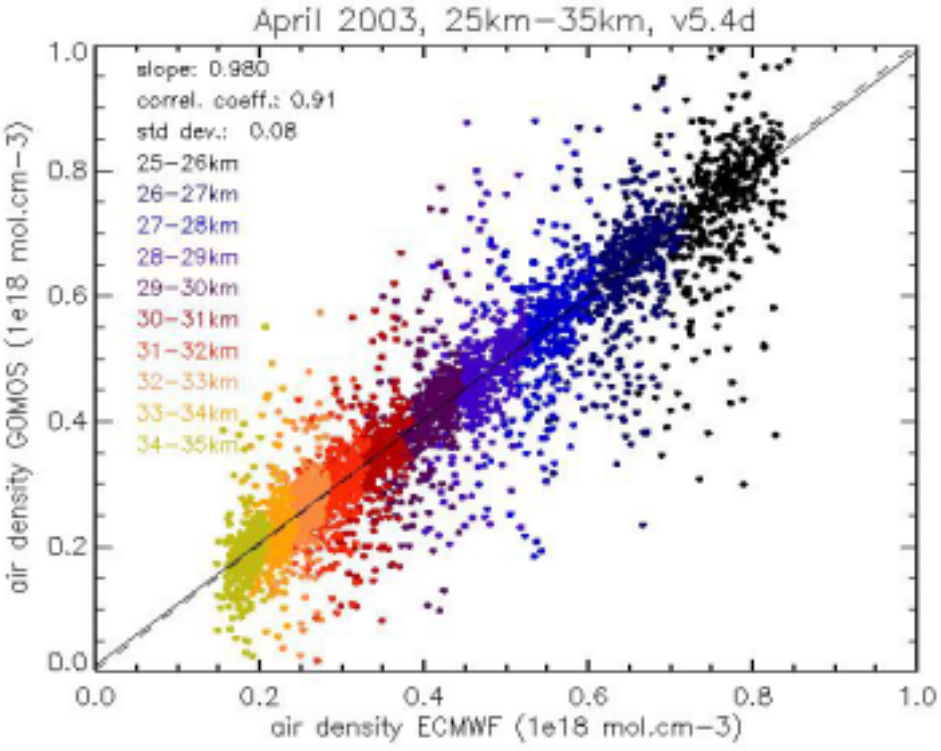

Figure 7.4-4: GOMOS air density vs ECMWF air density, April 2003, GOPR v5.4d

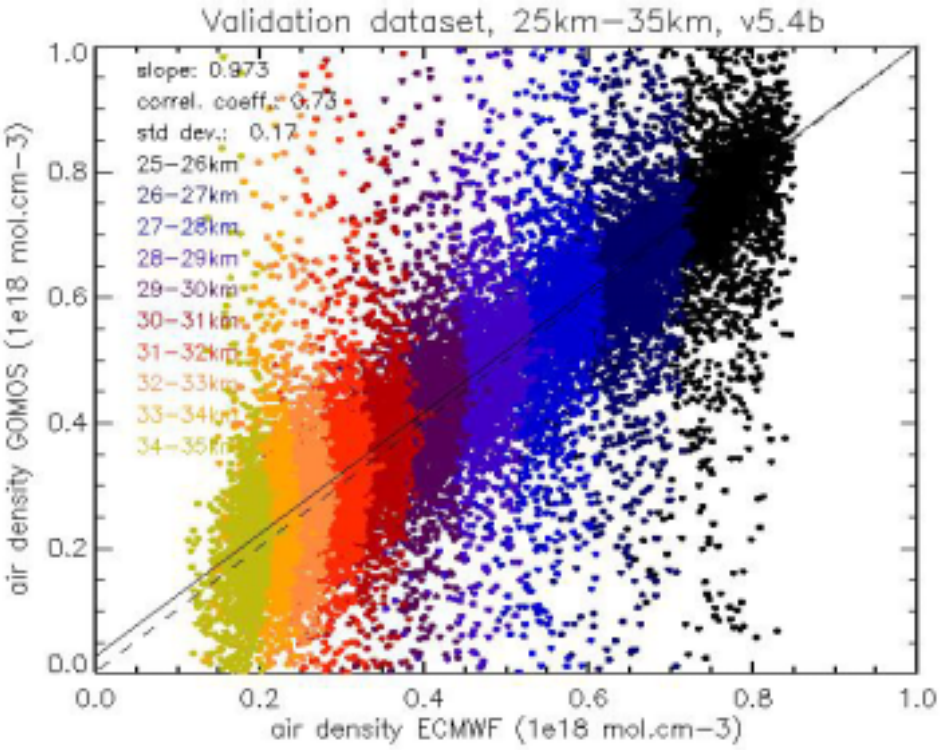

Figure 7.4-5: GOMOS air density vs ECMWF air density, Validation dataset, GOPR v5.4b

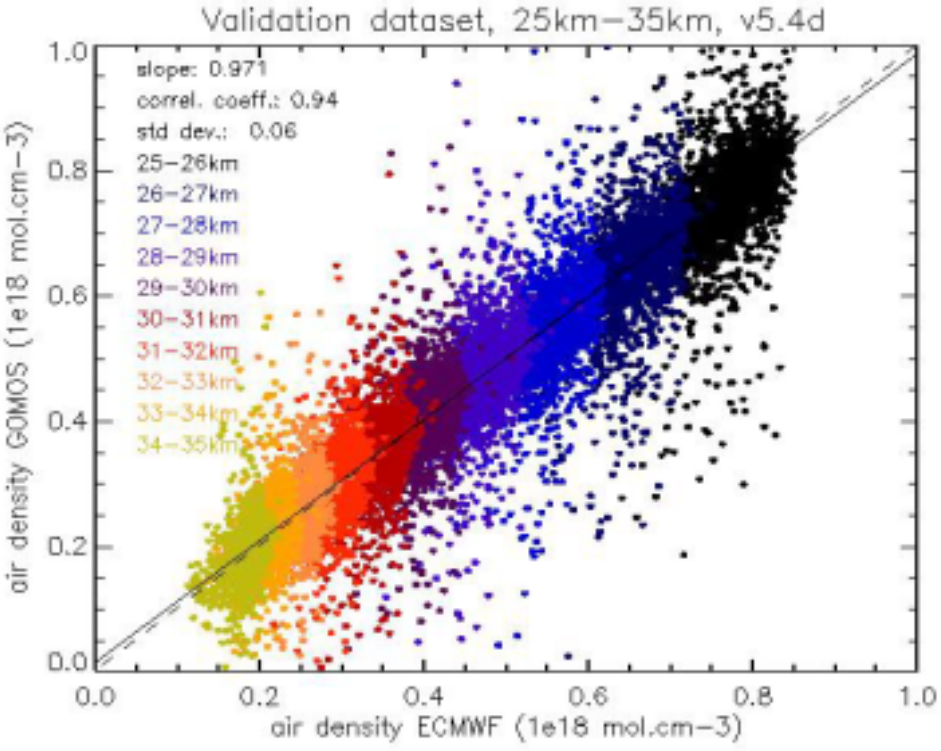

Figure 7.4-6: GOMOS air density vs ECMWF air density, Validation dataset, GOPR v5.4d